

Radiating Gravitational Collapse with Shearing Motion and Bulk Viscosity Revisited

G. Pinheiro and R. Chan

Observatório Nacional,

Coordenação de Astronomia e Astrofísica,

Rua General José Cristino 77,

São Cristóvão, CEP 20921-400,

Rio de Janeiro, Brazil

E-mail: gpinheiro@on.br, chan@on.br

(Dated: June 23, 2021)

Abstract

A new model is proposed to a collapsing star consisting of an anisotropic fluid with bulk viscosity, radial heat flow and outgoing radiation. In a previous paper one of us has introduced a function time dependent into the g_{rr} , besides the time dependent metric functions $g_{\theta\theta}$ and $g_{\phi\phi}$. The aim of this work is to generalize this previous model by introducing bulk viscosity and compare it to the non-viscous collapse. The behavior of the density, pressure, mass, luminosity and the effective adiabatic index is analyzed. Our work is also compared to the case of a collapsing fluid with bulk viscosity of another previous model, for a star with $6 M_{\odot}$. The pressure of the star, at the beginning of the collapse, is isotropic but due to the presence of the bulk viscosity the pressure becomes more and more anisotropic. The black hole is never formed because the apparent horizon formation condition is never satisfied, in contrast of the previous model where a black hole is formed. An observer at infinity sees a radial point source radiating exponentially until reaches the time of maximum luminosity and suddenly the star turns off. In contrast of the former model where the luminosity also increases exponentially, reaching a maximum and after it decreases until the formation of the black hole. The effective adiabatic index diminishes due to the bulk viscosity, thus increasing the instability of the system, in both models, in the former paper and in this work.

I. INTRODUCTION

One of the most outstanding problems in gravitation theory is the evolution of a collapsing massive star, after it has exhausted its nuclear fuel. The problem of constructing physically realistic models for radiating collapsing stars is one of the aims of the relativistic astrophysics. However, in order to obtain realistic models we need to solve complicated systems of nonlinear differential equations. In many cases we can simplify the problem considering some restrictions in these equations and solve the system analytically. Such models, although simplified, are useful to construct simple exact models, which are at least not physically unreasonable. This allows a clearer analysis of the main physical effects at play, and it can be very useful for checking of numerical procedures.

A great number of the previous works in gravitational collapse have considered only shear-free motion of the fluid [1–4]. This simplification allows us to obtain exact solutions of the Einstein's equations in some cases but it is somewhat unrealistic. It is also unrealistic to consider heat flow without viscosity but if viscosity is introduced, it is desirable to allow shear in the fluid motion.

In the work [5] the authors have studied the collapse of a radiating star with bulk viscosity but they still maintained the shear-free motion of the fluid. Thus, it is interesting to study solutions that contains shear, because it plays a very important role in the study of gravitational collapse, as shown in [6, 7, 9, 10, 12, 13] and in [14].

In the first paper [6, 7] we have compared two collapsing model: a shear-free and a shearing model. In this model we have imposed that the metric components g_{tt} and g_{rr} were independent of the time and only $g_{\theta\theta}$ and $g_{\phi\phi}$ were time dependent. We were interested in studying the effect of the shearing motion in the evolution of the collapse. It was shown that the pressure of the star, at the beginning of the collapse, is isotropic but due to the presence of the shear the pressure becomes more and more anisotropic. The anisotropy in self-gravitating systems has been reviewed and discussed the causes for its appearance by Herrera and Santos [15]. As shown by Chan [6, 7] the simplest cause of the presence of anisotropy in a self-gravitating body is the shearing motion of the fluid, because it appears without an imposition ad-hoc [4].

In the second work [9] we have used the same model of Chan [6, 7] and we have analyzed a collapsing radiating star consisting of an anisotropic fluid with shear viscosity undergoing

radial heat flow with outgoing radiation, but without bulk viscosity.

In the third paper [10] we have also used the same model previous papers [6] [7] and we have analyzed a collapsing radiating star consisting of an anisotropic fluid with bulk viscosity undergoing radial heat flow with outgoing radiation, but without shear viscosity.

In the fourth work [11] we have generalized our previous models by introducing a function time dependent into the g_{rr} and in a recent paper [13] we have introduced the shear viscosity.

The aim of this work is to generalize our previous model [10] by introducing a time dependent function into the g_{rr} , besides the time dependent metric functions $g_{\theta\theta}$ and $g_{\phi\phi}$, and to compare the physical results with the previous ones.

This work is organized as follows. In Section 2 we present the Einstein's field equations. In Section 3 we rederive the junction conditions, since in the former paper [13] have obtained only results without bulk viscosity. In Section 4 we present the proposed solution of the field equations. In Section 5 we describe the model considered in this work for the initial configuration. In Section 6 we present the energy conditions for a bulk viscous anisotropic fluid. In Section 7 we show the time evolution of the total mass, luminosity and the effective adiabatic index and in Section 8 we summarize the main results obtained in this work.

II. FIELD EQUATIONS

We assume a spherically symmetric distribution of fluid undergoing dissipation in the form of heat flow. While the dissipative fluid collapses it produces radiation. The interior spacetime is described by the most general spherically symmetric metric, using comoving coordinates,

$$ds_-^2 = -A^2(r, t)dt^2 + B^2(r, t)dr^2 + C^2(r, t)(d\theta^2 + \sin^2\theta d\phi^2). \quad (1)$$

The exterior spacetime is described by Vaidya's [16] metric, which represents an outgoing radial flux of radiation,

$$ds_+^2 = - \left[1 - \frac{2m(v)}{\mathbf{r}} \right] dv^2 - 2dv d\mathbf{r} + \mathbf{r}^2(d\theta^2 + \sin^2\theta d\phi^2), \quad (2)$$

where $m(v)$ represents the mass of the system inside the boundary surface Σ , function of the retarded time v .

We assume the interior energy-momentum tensor is given by

$$G_{\alpha\beta} = \kappa T_{\alpha\beta} = \kappa [(\mu + p_t)u_\alpha u_\beta + p_t g_{\alpha\beta} + (p - p_t)X_\alpha X_\beta + q_\alpha u_\beta + q_\beta u_\alpha - \zeta \Theta (g_{\alpha\beta} + u_\alpha u_\beta)], \quad (3)$$

where μ is the energy density of the fluid, p is the radial pressure, p_t is the tangential pressure, q^α is the radial heat flux, X_α is an unit four-vector along the radial direction, u^α is the four-velocity, which have to satisfy $u^\alpha q_\alpha = 0$, $X_\alpha X^\alpha = 1$, $X_\alpha u^\alpha = 0$ and $\kappa = 8\pi$ (i.e., $c = G = 1$). The quantity $\zeta > 0$ is the coefficient of bulk viscosity and the shearing tensor $\sigma_{\alpha\beta}$ is defined as

$$\sigma_{\alpha\beta} = u_{(\alpha;\beta)} + \dot{u}_{(\alpha}u_{\beta)} - \frac{1}{3}\Theta(g_{\alpha\beta} + u_\alpha u_\beta), \quad (4)$$

with

$$\dot{u}_\alpha = u_{\alpha;\beta}u^\beta, \quad (5)$$

$$\Theta = u_{;\alpha}^\alpha, \quad (6)$$

where the semicolon denotes a covariant derivative and the parentheses in the indices mean symmetrizations.

Since we utilize comoving coordinates we have,

$$u^\alpha = A^{-1}\delta_0^\alpha, \quad (7)$$

and since the heat flux is radial

$$q^\alpha = q\delta_1^\alpha. \quad (8)$$

Thus the non-zero components of the shearing tensor are given by

$$\sigma_{11} = \frac{2B^2}{3A} \left(\frac{\dot{B}}{B} - \frac{\dot{C}}{C} \right), \quad (9)$$

$$\sigma_{22} = -\frac{C^2}{3A} \left(\frac{\dot{B}}{B} - \frac{\dot{C}}{C} \right), \quad (10)$$

$$\sigma_{33} = \sigma_{22} \sin^2 \theta. \quad (11)$$

A simple calculation shows that

$$\sigma_{\alpha\beta}\sigma^{\alpha\beta} = \frac{2}{3A^2} \left(\frac{\dot{B}}{B} - \frac{\dot{C}}{C} \right)^2. \quad (12)$$

Thus, we define the scalar σ as

$$\sigma = -\frac{1}{3A} \left(\frac{\dot{B}}{B} - \frac{\dot{C}}{C} \right). \quad (13)$$

Using (1) and (6), we can write that

$$\Theta = \frac{1}{A} \left(\frac{\dot{B}}{B} + 2\frac{\dot{C}}{C} \right). \quad (14)$$

The non-vanishing components of the field equations, using (1), (3), (7), (8) and (14) , interior of the boundary surface Σ are

$$\begin{aligned} G_{00}^- &= -\left(\frac{A}{B}\right)^2 \left[2\frac{C''}{C} + \left(\frac{C'}{C}\right)^2 - 2\frac{C' B'}{C B} \right] \\ &\quad + \left(\frac{A}{C}\right)^2 + \frac{\dot{C}}{C} \left(\frac{\dot{C}}{C} + 2\frac{\dot{B}}{B} \right) = \kappa A^2 \mu, \end{aligned} \quad (15)$$

$$\begin{aligned} G_{11}^- &= \frac{C'}{C} \left(\frac{C'}{C} + 2\frac{A'}{A} \right) - \left(\frac{B}{C} \right)^2 \\ &\quad - \left(\frac{B}{A} \right)^2 \left[2\frac{\ddot{C}}{C} + \left(\frac{\dot{C}}{C} \right)^2 - 2\frac{\dot{A}\dot{C}}{AC} \right] \\ &= \kappa B^2 (p - \zeta \Theta), \end{aligned} \quad (16)$$

$$\begin{aligned} G_{22}^- &= \left(\frac{C}{B} \right)^2 \left[\frac{C''}{C} + \frac{A''}{A} + \frac{C' A'}{C A} - \frac{A' B'}{A B} - \frac{B' C'}{B C} \right] \\ &\quad + \left(\frac{C}{A} \right)^2 \left[-\frac{\ddot{B}}{B} - \frac{\ddot{C}}{C} - \frac{\dot{C}\dot{B}}{CB} + \frac{\dot{A}\dot{C}}{AC} + \frac{\dot{A}\dot{B}}{AB} \right] \\ &= \kappa C^2 (p_t - \zeta \Theta), \end{aligned} \quad (17)$$

$$G_{33}^- = G_{22}^- \sin^2 \theta, \quad (18)$$

$$G_{01}^- = -2\frac{\dot{C}'}{C} + 2\frac{C'}{C} \frac{\dot{B}}{B} + 2\frac{A'}{A} \frac{\dot{C}}{C} = -\kappa AB^2 q. \quad (19)$$

The dot and the prime stand for differentiation with respect to t and r , respectively.

III. JUNCTION CONDITIONS

We consider a spherical surface with its motion described by a time-like three-space Σ , which divides spacetimes into interior and exterior manifolds. For the junction conditions we follow the approach given by Israel [17, 18]. Hence we have to demand

$$(ds_-^2)_\Sigma = (ds_+^2)_\Sigma, \quad (20)$$

$$K_{ij}^- = K_{ij}^+, \quad (21)$$

where K_{ij}^\pm is the extrinsic curvature to Σ , given by

$$K_{ij}^\pm = -n_\alpha^\pm \frac{\partial^2 x^\alpha}{\partial \xi^i \partial \xi^j} - n_\alpha^\pm \Gamma_{\beta\gamma}^\alpha \frac{\partial x^\beta}{\partial \xi^i} \frac{\partial x^\gamma}{\partial \xi^j}, \quad (22)$$

and where $\Gamma_{\beta\gamma}^\alpha$ are the Christoffel symbols, n_α^\pm the unit normal vectors to Σ , x^α are the coordinates of interior and exterior spacetimes and ξ^i are the coordinates that define the surface Σ .

From the junction condition (20) we obtain

$$\frac{dt}{d\tau} = A(r_\Sigma, t)^{-1}, \quad (23)$$

$$C(r_\Sigma, t) = \mathbf{r}_\Sigma(v), \quad (24)$$

$$\left(\frac{dv}{d\tau}\right)_\Sigma^{-2} = \left(1 - \frac{2m}{\mathbf{r}} + 2\frac{d\mathbf{r}}{dv}\right)_\Sigma, \quad (25)$$

where τ is a time coordinate defined only on Σ .

The unit normal vectors to Σ (for details see [19]) are given by

$$n_\alpha^- = B(r_\Sigma, t)\delta_\alpha^1, \quad (26)$$

$$n_\alpha^+ = \left(1 - \frac{2m}{\mathbf{r}} + 2\frac{d\mathbf{r}}{dv}\right)_\Sigma^{-1/2} \left(-\frac{d\mathbf{r}}{dv}\delta_\alpha^0 + \delta_\alpha^1\right)_\Sigma. \quad (27)$$

The non-vanishing extrinsic curvature are given by

$$K_{\tau\tau}^- = - \left[\left(\frac{dt}{d\tau} \right)^2 \frac{A'A}{B} \right]_{\Sigma}, \quad (28)$$

$$K_{\theta\theta}^- = \left(\frac{C'C}{B} \right)_{\Sigma}, \quad (29)$$

$$K_{\phi\phi}^- = K_{\theta\theta}^- \sin^2 \theta, \quad (30)$$

$$K_{\tau\tau}^+ = \left[\frac{d^2 v}{d\tau^2} \left(\frac{dv}{d\tau} \right)^{-1} - \left(\frac{dv}{d\tau} \right) \frac{m}{\mathbf{r}^2} \right]_{\Sigma}, \quad (31)$$

$$K_{\theta\theta}^+ = \left[\left(\frac{dv}{d\tau} \right) \left(1 - \frac{2m}{\mathbf{r}} \right) \mathbf{r} + \frac{d\mathbf{r}}{d\tau} \mathbf{r} \right]_{\Sigma}, \quad (32)$$

$$K_{\phi\phi}^+ = K_{\theta\theta}^+ \sin^2 \theta. \quad (33)$$

From the equations (29) and (32) we have

$$\left[\left(\frac{dv}{d\tau} \right) \left(1 - \frac{2m}{\mathbf{r}} \right) \mathbf{r} + \frac{d\mathbf{r}}{d\tau} \mathbf{r} \right]_{\Sigma} = \left(\frac{C'C}{B} \right)_{\Sigma}. \quad (34)$$

With the help of equations (23), (24), (25), we can write (34) as

$$m = \left\{ \frac{C}{2} \left[1 + \left(\frac{\dot{C}}{A} \right)^2 - \left(\frac{C'}{B} \right)^2 \right] \right\}_{\Sigma}, \quad (35)$$

which is the total energy entrapped inside the surface Σ [20].

From the equations (28) and (31), using (23), we have

$$\left[\frac{d^2 v}{d\tau^2} \left(\frac{dv}{d\tau} \right)^{-1} - \left(\frac{dv}{d\tau} \right) \frac{m}{\mathbf{r}^2} \right]_{\Sigma} = - \left(\frac{A'}{AB} \right)_{\Sigma}. \quad (36)$$

Substituting equations (23), (24) and (35) into (34) we can write

$$\left(\frac{dv}{d\tau} \right)_{\Sigma} = \left(\frac{C'}{B} + \frac{\dot{C}}{A} \right)_{\Sigma}^{-1}. \quad (37)$$

Differentiating (37) with respect to τ and using equations (35), (37), we can rewrite (36)

as

$$\begin{aligned}
& \left(\frac{C}{2AB} \right)_\Sigma \left\{ 2 \frac{\dot{C}'}{C} - 2 \frac{C'}{C} \frac{\dot{B}}{B} - 2 \frac{A'}{A} \frac{\dot{C}}{C} + \right. \\
& \left. \left(\frac{B}{A} \right) \left[2 \frac{\ddot{C}}{C} - 2 \frac{\dot{C}}{C} \frac{\dot{A}}{A} + \left(\frac{A}{C} \right)^2 + \left(\frac{\dot{C}}{C} \right)^2 - \right. \right. \\
& \left. \left. \left(\frac{A}{B} \right)^2 \left(\frac{C'}{C} \right)^2 - \left(\frac{A}{B} \right)^2 \left(2 \frac{A' C'}{A C} \right) \right] \right\} = 0. \tag{38}
\end{aligned}$$

Comparing (38) with (16) and (19), we can finally write

$$(p - \zeta\Theta)_\Sigma = (qB)_\Sigma. \tag{39}$$

This result is analogous to the one obtained by Chan [11] for a shearing fluid motion but now we have generalized for an interior fluid with bulk viscosity.

The total luminosity for an observer at rest at infinity is

$$L_\infty = - \left(\frac{dm}{dv} \right)_\Sigma = - \left[\frac{dm}{dt} \frac{dt}{d\tau} \left(\frac{dv}{d\tau} \right)^{-1} \right]_\Sigma. \tag{40}$$

Differentiating (35) with respect to t , using (23), (37) and (16), we obtain that

$$L_\infty = \frac{\kappa}{2} \left[(p - \zeta\Theta) C^2 \left(\frac{C'}{B} + \frac{\dot{C}}{A} \right)^2 \right]_\Sigma. \tag{41}$$

The boundary redshift can be used to determine the time of formation of the horizon.

The boundary redshift z_Σ is given by

$$\left(\frac{dv}{d\tau} \right)_\Sigma = 1 + z_\Sigma. \tag{42}$$

The redshift, for an observer at rest at infinity diverges at the time of formation of the black hole. From (37) we can see that this happens when

$$\left(\frac{C'}{B} + \frac{\dot{C}}{A} \right)_\Sigma = 0. \tag{43}$$

IV. SOLUTION OF THE FIELD EQUATIONS

Again as in former paper [11] we propose solutions of the field equations (15)-(19) with the form

$$A(r, t) = A_0(r), \quad (44)$$

$$B(r, t) = B_0(r)h(t), \quad (45)$$

$$C(r, t) = rB_0(r)f(t). \quad (46)$$

We have chosen this separation of variables in the metric functions, in order to have the following properties: (a) when $h(t) \rightarrow 1$ and $f(t) \rightarrow 1$ the metric functions represent the static solution of the initial star configuration; (b) when $h(t) = f(t)$ the metric functions represent the shear-free solution. We also remark that, following the junction condition equation (24), the function $C(r_\Sigma, t)$ represents the luminosity radius of the body as seen by an exterior observer. On the other hand, with this solution the proper radius $\int_0^r B(r, t)dr$ evolve with the time. Such a property was not present in the previous models [6] [7] [9] [10] [12].

Thus, the expansion scalar (14) can be written as

$$\Theta = \frac{1}{A_0} \left(\frac{\dot{h}}{h} + 2\frac{\dot{f}}{f} \right). \quad (47)$$

Now the equations (15)-(19) can be written as

$$\kappa\mu = \kappa\frac{\mu_0}{h^2} + \frac{1}{A_0^2} \left(\frac{\dot{f}}{f} \right) \left(\frac{\dot{f}}{f} + 2\frac{\dot{h}}{h} \right) + \frac{1}{r^2 B_0^2} \left(\frac{1}{f^2} - \frac{1}{h^2} \right), \quad (48)$$

$$\kappa p = \kappa\frac{p_0}{h^2} - \frac{1}{A_0^2} \left[2\frac{\ddot{f}}{f} + \left(\frac{\dot{f}}{f} \right)^2 \right] - \frac{1}{r^2 B_0^2} \left(\frac{1}{f^2} - \frac{1}{h^2} \right) + \frac{\kappa\zeta}{A_0} \left(\frac{2\dot{f}}{f} + \frac{\dot{h}}{h} \right) \quad (49)$$

$$\kappa p_t = \kappa\frac{p_0}{h^2} - \frac{1}{A_0^2} \left(\frac{\ddot{f}}{f} + \frac{\ddot{h}}{h} + \frac{\dot{h}\dot{f}}{hf} \right) + \frac{\kappa\zeta}{A_0} \left(\frac{2\dot{f}}{f} + \frac{\dot{h}}{h} \right) \quad (50)$$

$$\begin{aligned} \kappa q = \frac{2}{A_0 B_0^2 h^2} & \left[\left(\frac{\dot{f}}{f} \right) \left(\frac{B'_0}{B_0} + \frac{1}{r} - \frac{A'_0}{A_0} \right) - \right. \\ & \left. - \left(\frac{\dot{h}}{h} \right) \left(\frac{B'_0}{B_0} + \frac{1}{r} \right) \right], \end{aligned} \quad (51)$$

where

$$\kappa \mu_0 = -\frac{1}{B_0^2} \left[2 \frac{B''_0}{B_0} - \left(\frac{B'_0}{B_0} \right)^2 + \frac{4 B'_0}{r B_0} \right], \quad (52)$$

$$\kappa p_0 = \frac{1}{B_0^2} \left[\left(\frac{B'_0}{B_0} \right)^2 + \frac{2 B'_0}{r B_0} + 2 \frac{A'_0 B'_0}{A_0 B_0} + \frac{2 A'_0}{r A_0} \right]. \quad (53)$$

We can see from equations (48)-(51) that when the functions $h(t) = 1$ and $f(t) = 1$ we obtain the static perfect fluid configuration.

Substituting equations (49) and (51) into (39), assuming also that $p_0(r_\Sigma) = 0$, we obtain a second order differential equation in $h(t)$ and $f(t)$,

$$2 \frac{\ddot{f}}{f} + \left(\frac{\dot{f}}{f} \right)^2 + \frac{1}{h} \left[a \left(\frac{\dot{f}}{f} \right) - \bar{a} \left(\frac{\dot{h}}{h} \right) \right] + b \left(\frac{1}{f^2} - \frac{1}{h^2} \right) = 0, \quad (54)$$

where

$$a = \left[2 \left(\frac{A_0}{B_0} \right) \left(\frac{B'_0}{B_0} + \frac{1}{r} - \frac{A'_0}{A_0} \right) \right]_\Sigma, \quad (55)$$

$$\bar{a} = \left[2 \left(\frac{A_0}{B_0} \right) \left(\frac{B'_0}{B_0} + \frac{1}{r} \right) \right]_\Sigma, \quad (56)$$

and

$$b = \left(\frac{A_0^2}{r^2 B_0^2} \right)_\Sigma. \quad (57)$$

In order to obtain the quantities (48)-(51) we have first to find an appropriate $h(t)$ function. Let us first assume that $f(t) = 1$. Thus, we obtain the differential equation for $h(t)$ given by

$$a_0 \dot{h} - h^2 + 1 = 0, \quad (58)$$

where $a_0 = \bar{a}/b$ and whose solution is given by [8]

$$h(t) = -\tanh \left(\frac{t}{a_0} \right). \quad (59)$$

Now, using equation (58) we can write equation (54) in the following way

$$2f\ddot{f} + \dot{f}^2 + a(f/h)\dot{f} + b(1 - f^2) = 0. \quad (60)$$

This equation is almost identical to the one obtained previously [6] [7] [9] [10] [12], except the factor $(1/h)$ in the third term. Thus, as before it has to be solved numerically, assuming that at $t \rightarrow -\infty$ represents the static configuration with $\dot{f}(t \rightarrow -\infty) \rightarrow 0$ and $f(t \rightarrow -\infty) \rightarrow 1$. We also assume that $f(t \rightarrow 0) \rightarrow 0$. This means that the luminosity radius $C(r_\Sigma, t)$ has the value $r_\Sigma B_0(r_\Sigma)$ at the beginning of the collapse and vanishing at the end of the evolution. Analogously, the proper radius has the value $h(t) \int_0^r B_0(r) dr$ at the beginning of the collapse and also vanishing at the end of the collapse.

V. MODEL OF THE INITIAL CONFIGURATION

We consider that the system at the beginning of the collapse has a static configuration of a perfect fluid satisfying the Schwarzschild interior solution [21]

$$A_0 = \frac{g(r)}{2(1 + r_\Sigma^2)(1 + r^2)}, \quad (61)$$

$$B_0 = \frac{2R}{1 + r^2}, \quad (62)$$

where

$$g(r) = 3(1 - r_\Sigma^2)(1 + r^2) - (1 + r_\Sigma^2)(1 - r^2), \quad (63)$$

and

$$R = m_0 \frac{(1 + r_\Sigma^2)^3}{4r_\Sigma^3}. \quad (64)$$

and where r_Σ is the radial coordinate relative to the physical initial radius of the star in comoving coordinates and m_0 is the initial mass of the system. Thus the static uniform energy density and static pressure are given by

$$\kappa\mu_0 = \frac{3}{R^2}, \quad (65)$$

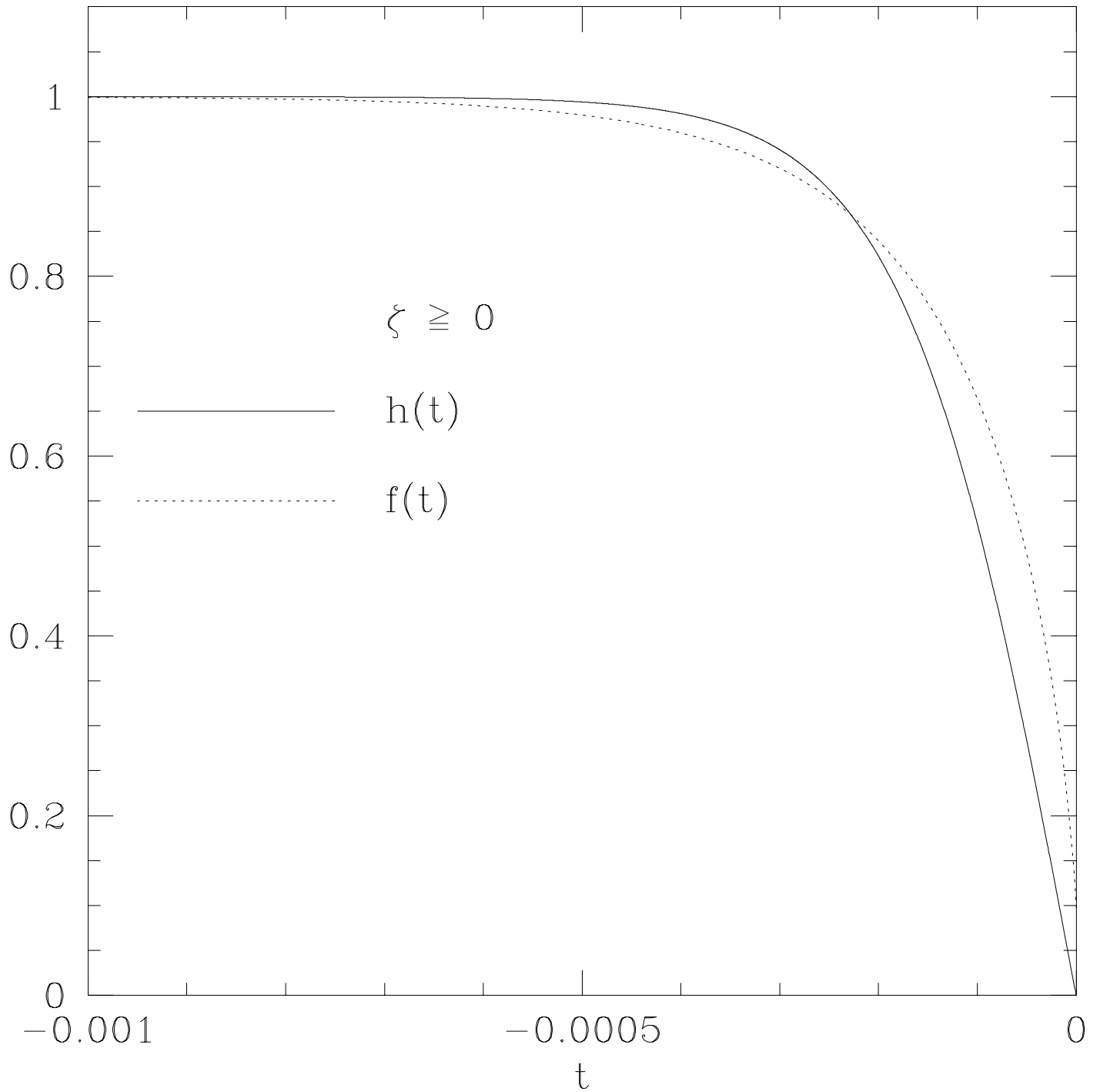


FIG. 1: Time behavior of the functions $f(t)$ and $h(t)$ for the model with or without bulk viscosity. The time is in units of second and $f(t)$ and $h(t)$ are dimensionless. The symbols $\zeta \geq 0$ mean that the plotted quantity is independent of ζ .

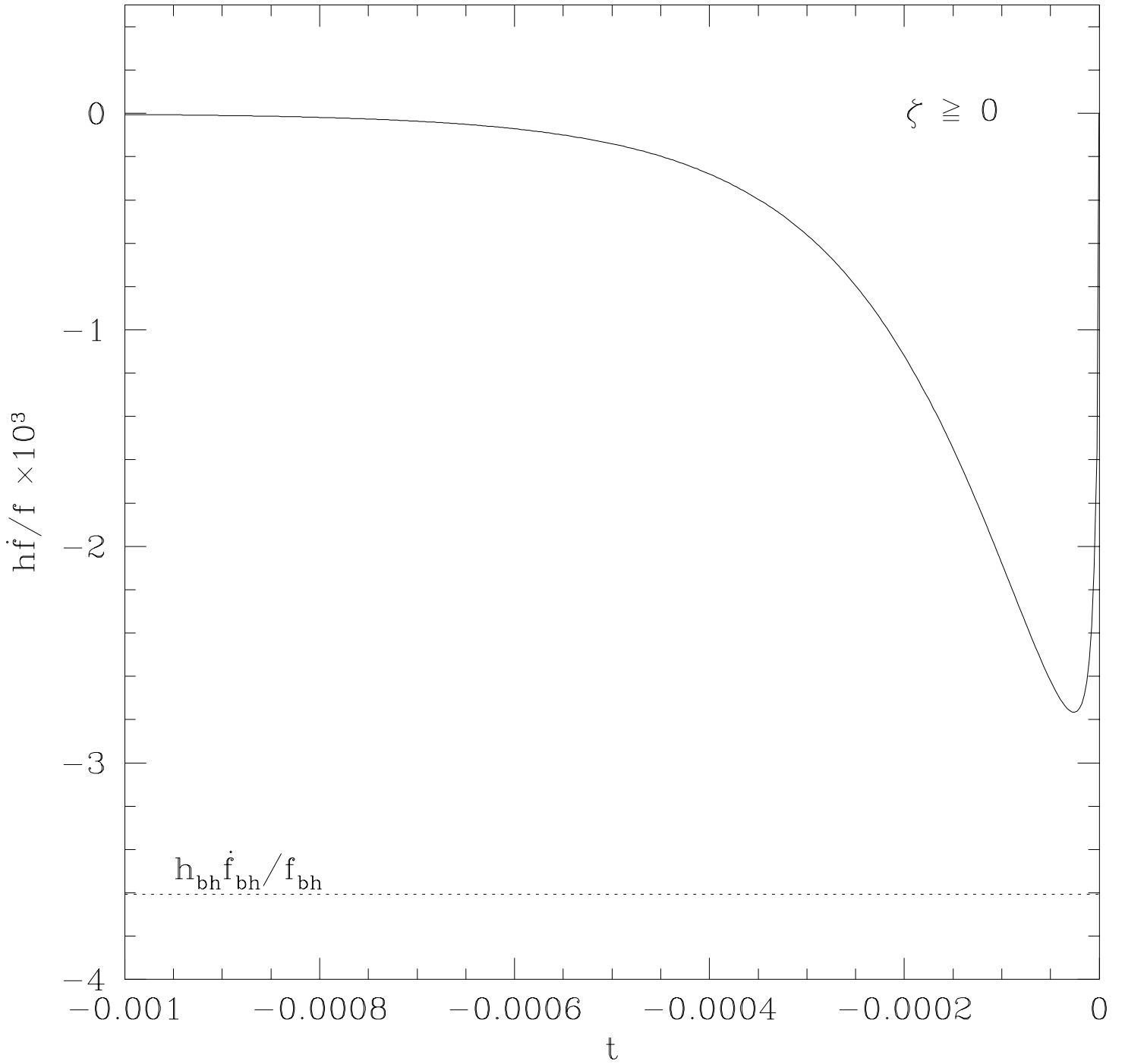


FIG. 2: The function $h\dot{f}/f$ as a function of the time. The time is in units of second. The symbols $\zeta \geq 0$ mean that the plotted quantity is independent of ζ .

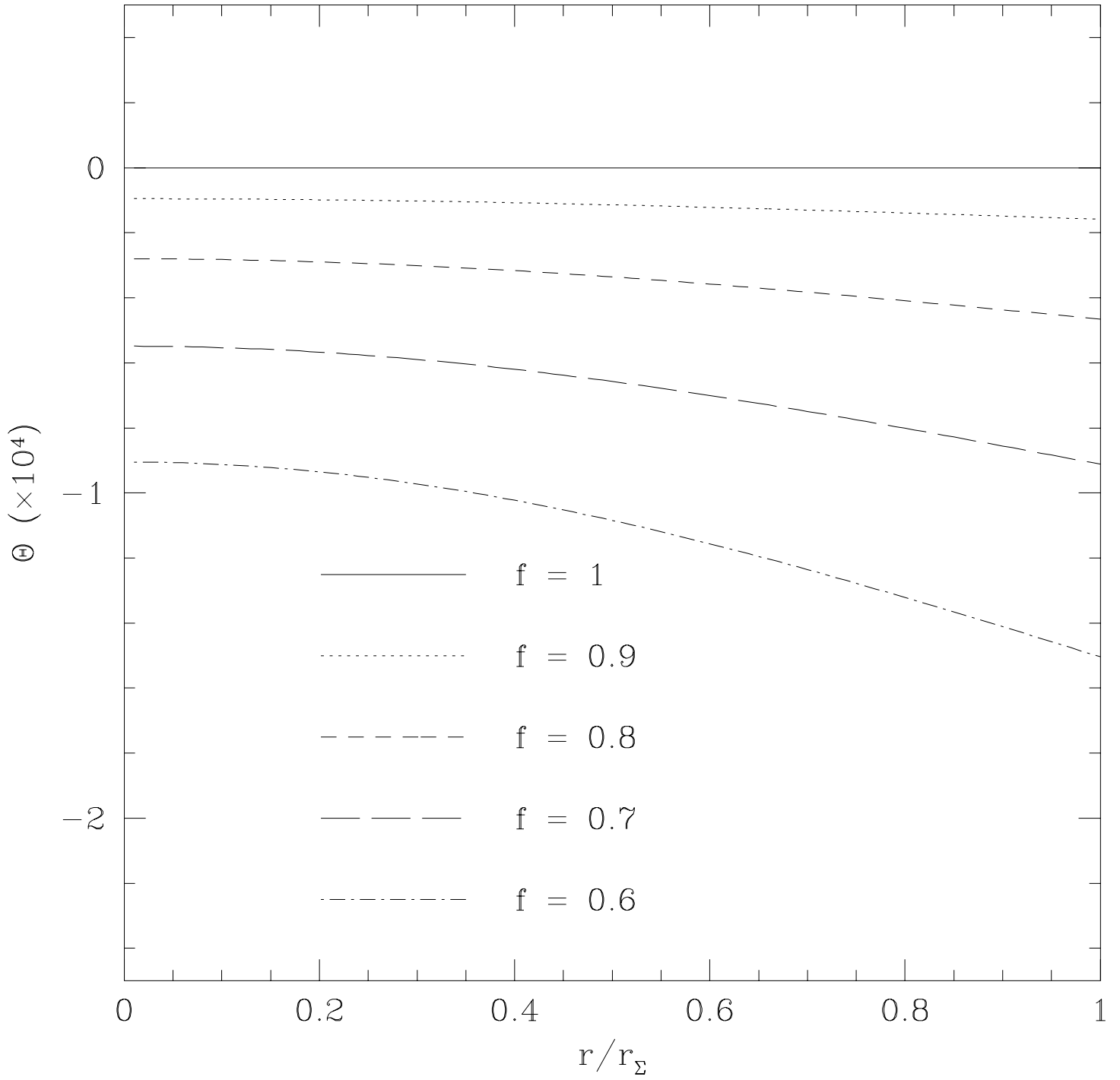


FIG. 3: The expansion scalar profiles as a function of the time. The radial coordinates r and r_Σ are in units of second.

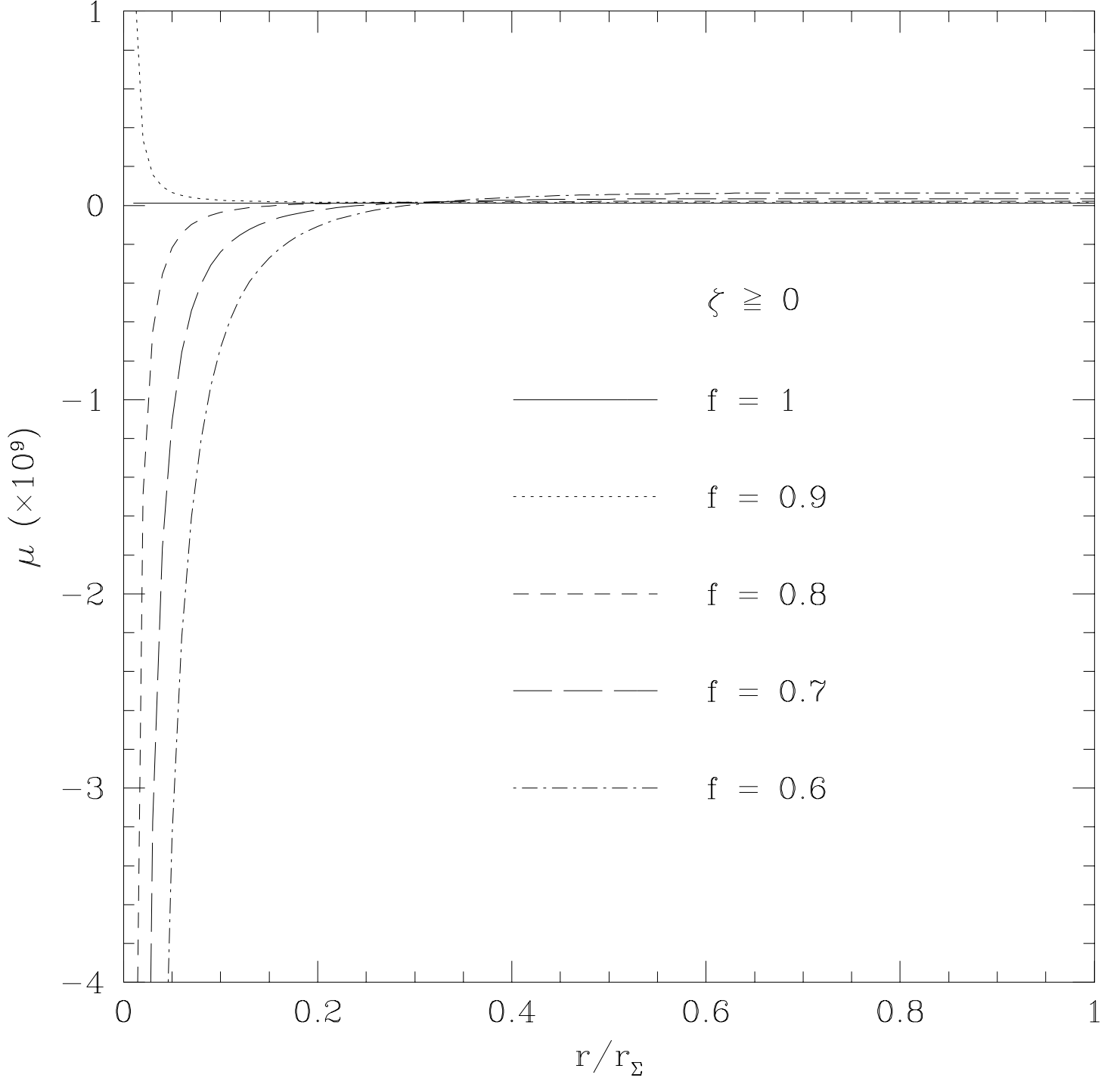


FIG. 4: Density profiles for the model with or without bulk viscosity. The radial coordinates r and r_Σ are in units of seconds and the density is in units of sec^{-2} . The symbols $\zeta \geq 0$ mean that the plotted quantity is independent of ζ .

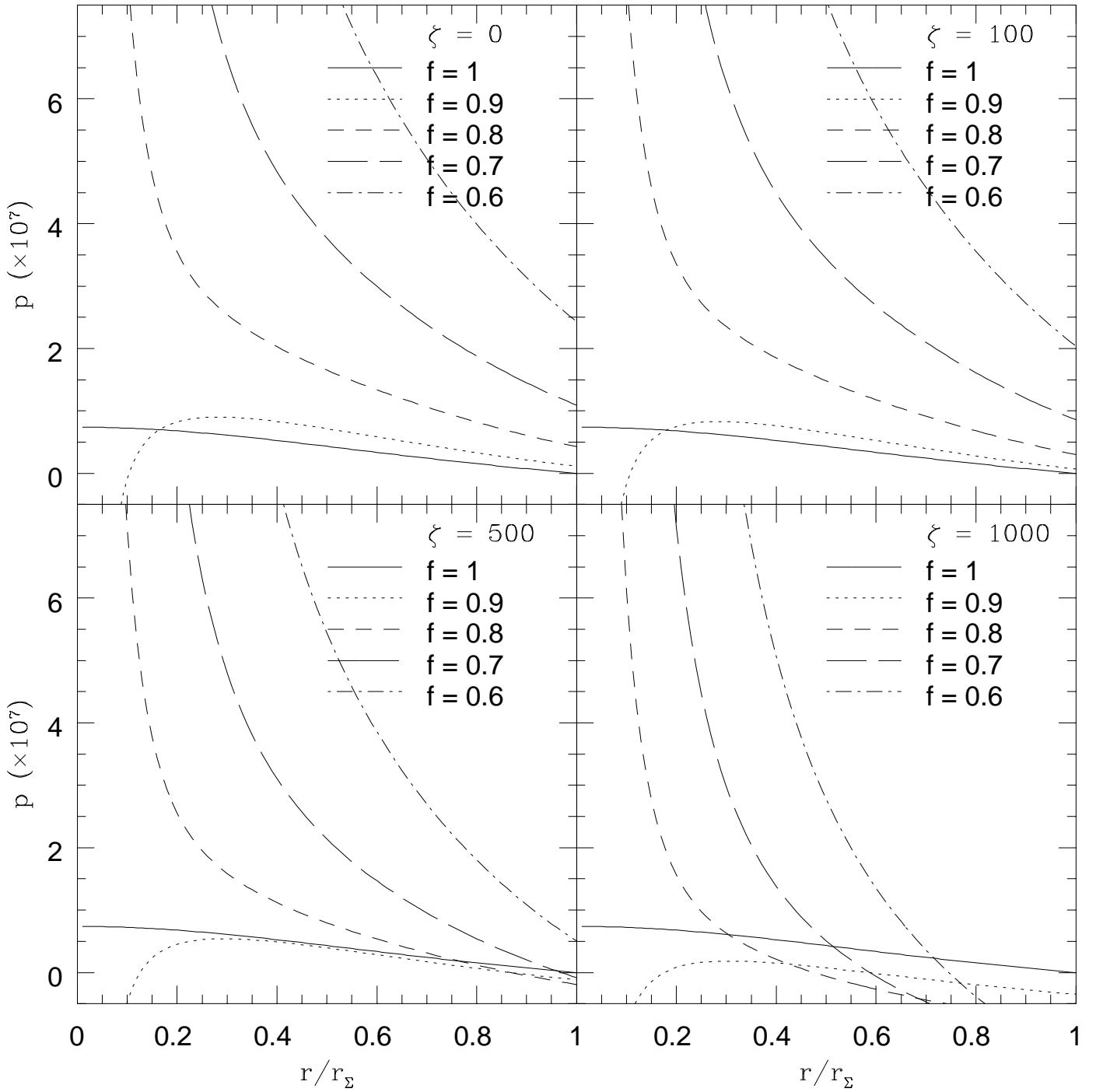


FIG. 5: Radial pressure profiles for four different values of ζ . The radial coordinates r and r_Σ are in units of seconds and the radial pressure is in units of sec^{-2} .

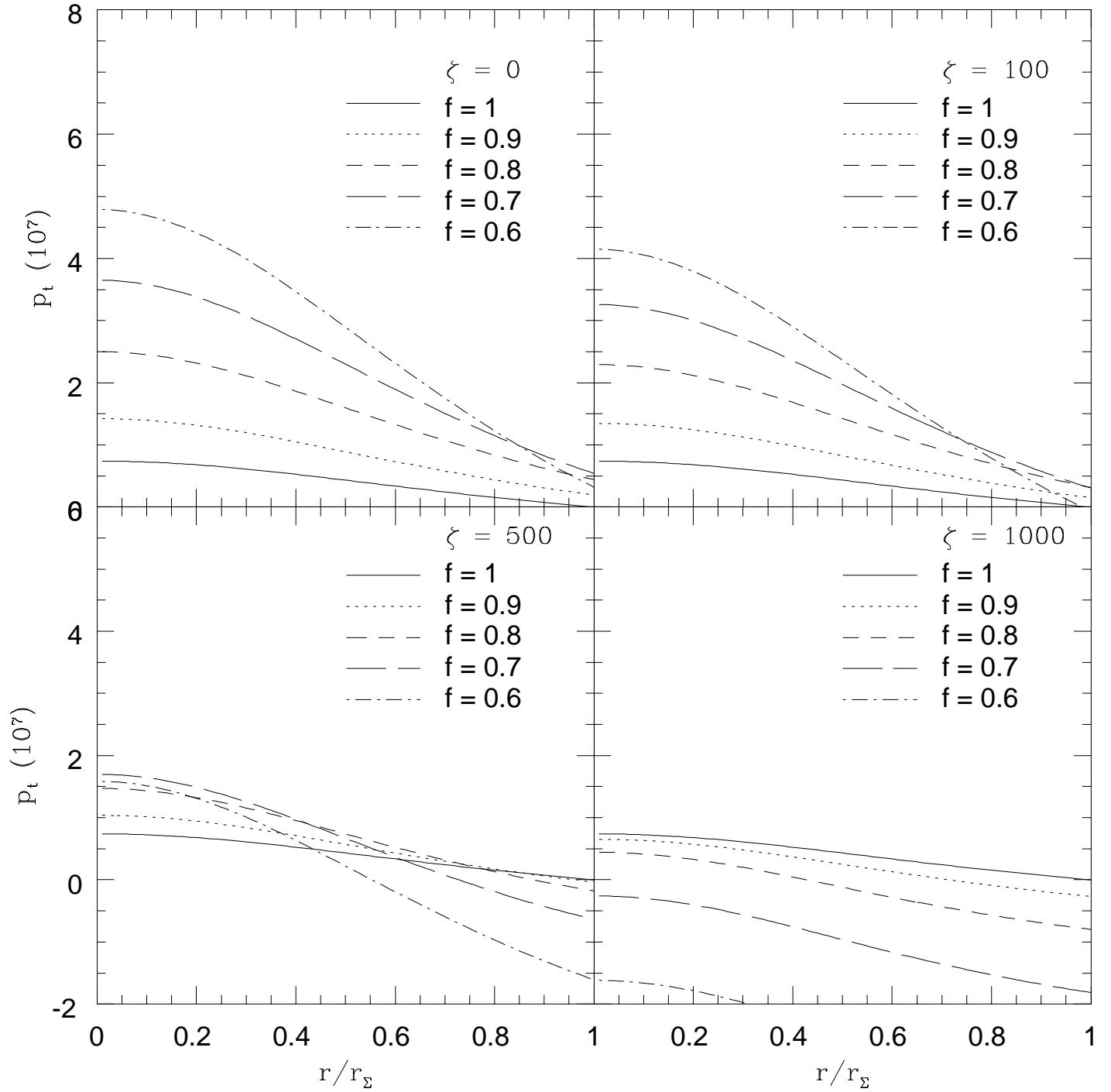


FIG. 6: Tangential pressure profiles for four different values of ζ . The radial coordinates r and r_Σ are in units of seconds and the tangential pressure p_t is in units of sec^{-2} .

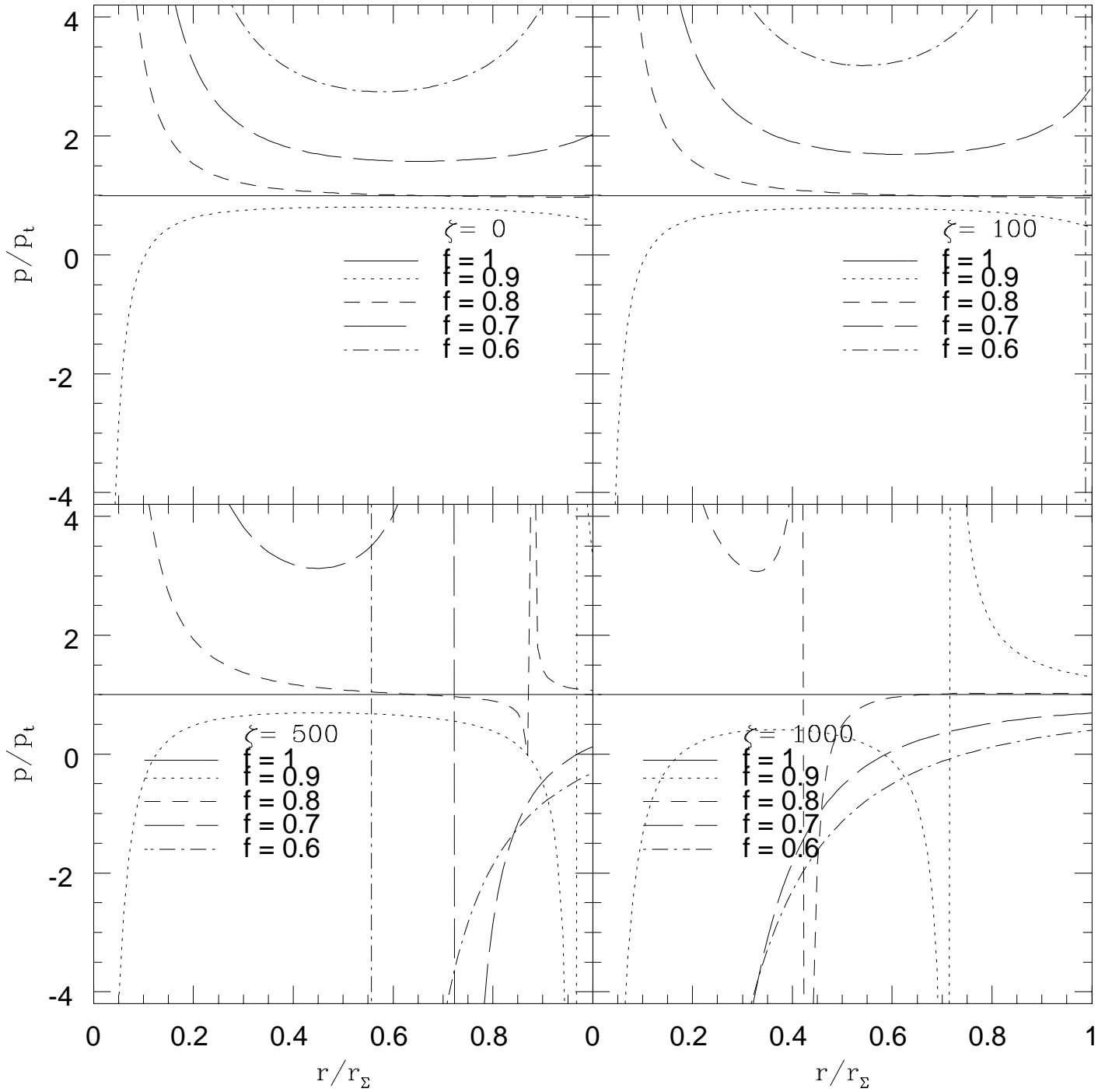


FIG. 7: The profiles for four different values of ζ of the ratio between the radial and tangential pressures. The radial coordinates r and r_Σ are in units of seconds; and the radial and tangential pressure, p and p_t , are in units of sec^{-2} .

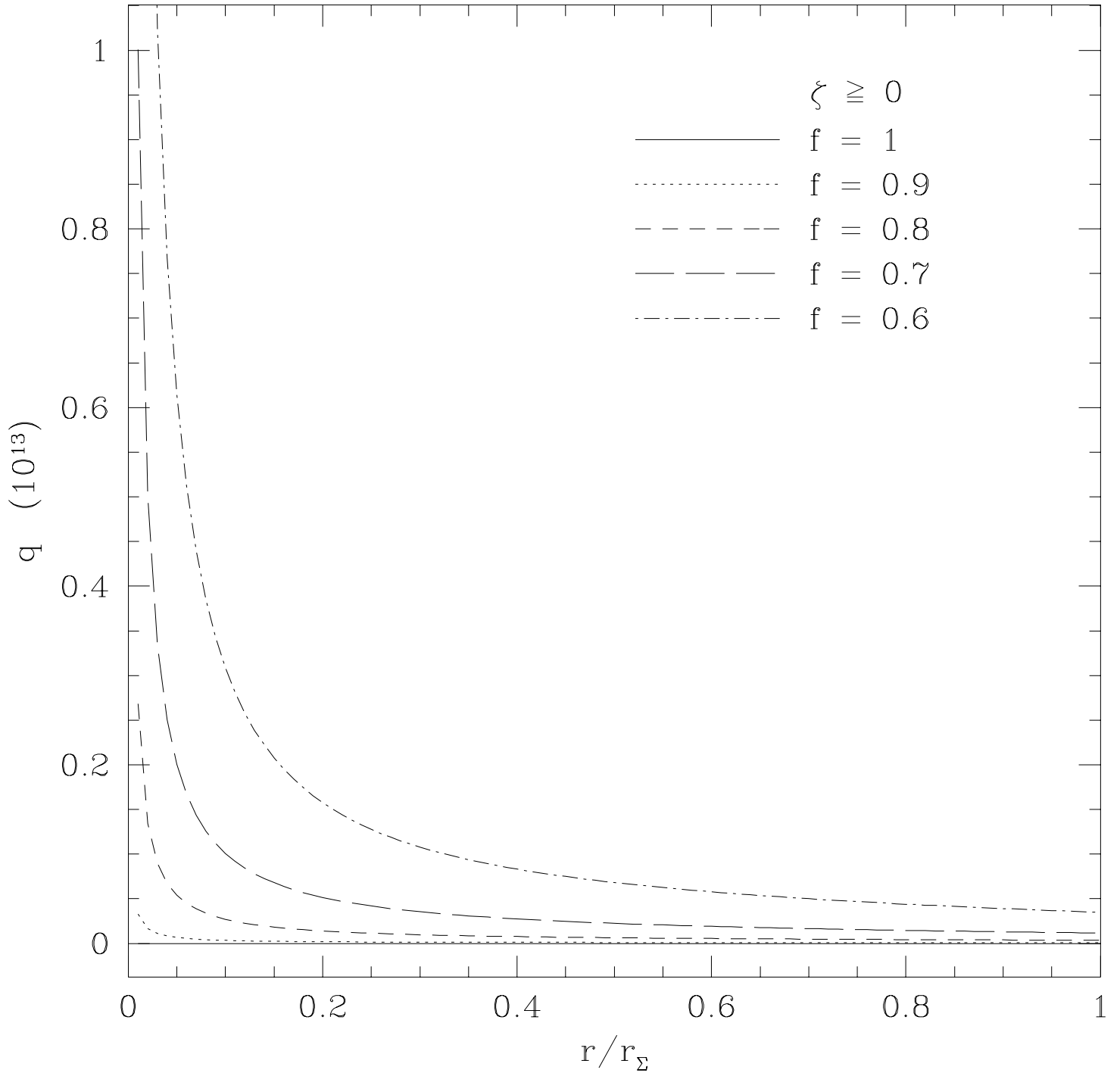


FIG. 8: Heat flux scalar profiles for the model with or without bulk viscosity. The radial coordinate r and r_Σ are in units of seconds and the heat flux q is in units of sec^{-2} . The symbols $\zeta \geq 0$ mean that the plotted quantity is independent of ζ .

$$\kappa p_0 = \frac{6}{R^2} \frac{(r_\Sigma^2 - r^2)}{g(r)}. \quad (66)$$

We consider the initial configuration as due to a iron core of a presupernova with $m_0 = 6M_\odot$, initial radial coordinate $r_\Sigma = 1.6 \times 10^5$ km, which correspond to 2.963×10^{-5} and 5.337×10^{-1} , respectively, in units of second. Thus, the physical radius $r_\Sigma B_0(r_\Sigma) = 25.742$ km, which gives a density of 1.675×10^{14} g cm⁻³ [22]. With these values we can solve numerically the differential equation (60). We can see from (51), using (61)-(64) and this initial configuration, that $[(B'_0/B_0 + 1/r - A'_0/A_0)/A_0]_\Sigma < 0$, $(B'_0/B_0 + 1/r)_\Sigma > 0$, $\dot{g} < 0$ and by the fact that $q_\Sigma > 0$ then we conclude that $\dot{f} < 0$. In figure 1 we can see the time evolution of the functions $f(t)$ and $h(t)$.

In order to determine the time of formation of the horizon f_{bh} , we use the equations (43), (44)-(46), (61)-(66) and write

$$\frac{\dot{f}_{\text{bh}}}{f_{\text{bh}}} h_{\text{bh}} = -\frac{2r_\Sigma^2(1 - r_\Sigma^2)^2}{m_0(1 + r_\Sigma^2)^4} \approx -3.606 \times 10^3. \quad (67)$$

Using the numerical solution of $f(t)$, $h(t)$ and equation (67), we can see from figure 2 that the horizon is never formed, because the function $hf\dot{f}/f$ does not reach the value -3.606×10^3 . At the first sight this fact could be interpreted as the formation of a naked singularity. However, this is not the case as we will see below in the calculation of the total energy entrapped inside the hypersurface Σ .

We will assume that ζ is constant, but in general the bulk viscosity coefficient depends on the temperature and density of the fluid [23]. The dependence of the expansion scalar on the time and radial coordinate is shown in the figure 3. Hereinafter, the values of ζ will be 1.347×10^{30} , 6.736×10^{30} and 1.347×10^{31} g cm⁻¹ s⁻¹, which correspond to values 100, 500 and 1000 s⁻¹, respectively, in time units. These values are about ten orders of magnitude above current estimates of the bulk viscosity coefficient in neutron stars [24]. If these lower values were used in our model, we would have obtained results like the ones with $\zeta \approx 0$, i.e., without bulk viscosity.

It is shown in figures 4 and 8 the radial profiles of the density and the heat flux. It is shown only one plot for each quantity because they do not depend on the bulk viscosity, which can be seen from equations (48) and (51).

In figure 5 and 6 we notice that the radial and tangential pressures diminish with the

bulk viscosity.

In the figure 7 ($\zeta = 0$) we can see that the star is isotropic at the beginning of the collapse ($f = 1$) but becoming more and more anisotropic at later times.

VI. ENERGY CONDITIONS FOR A VISCOUS ANISOTROPIC FLUID

Following the same procedure used in Kolassis, Santos and Tsoubelis [25] we can generalize the energy conditions for a viscous anisotropic fluid.

For the energy-momentum tensor Segre type $[111, 1]$ and if λ_0 denotes the eigenvalue corresponding to the timelike eigenvector, the general energy conditions are equivalent to the following relations between the eigenvalues of the energy-momentum tensor:

a) weak energy condition

$$-\lambda_0 \geq 0, \quad (68)$$

and

$$-\lambda_0 + \lambda_i \geq 0, \quad (69)$$

b) dominant energy condition

$$\lambda_0 \leq \lambda_i \leq -\lambda_0, \quad (70)$$

c) strong energy condition

$$-\lambda_0 + \sum_i \lambda_i \geq 0, \quad (71)$$

and

$$-\lambda_0 + \lambda_i \geq 0, \quad (72)$$

where the values $i = 1, 2, 3$ represent the eigenvalues corresponding to the spacelike eigenvectors.

The eigenvalues λ of the energy-momentum tensor are the roots of the equation

$$|T_{\alpha\beta} - \lambda g_{\alpha\beta}| = 0. \quad (73)$$

Thus, we can rewrite equation (73) as

$$\begin{vmatrix} A^2(\mu + \lambda) & -AB\bar{q} & 0 & 0 \\ -AB\bar{q} & B^2(p - \lambda - \zeta\Theta) & 0 & 0 \\ 0 & 0 & C^2(p_t - \lambda - \zeta\Theta) & 0 \\ 0 & 0 & 0 & C^2(p_t - \lambda - \zeta\Theta) \end{vmatrix} = 0,$$

where $\bar{q} = qB$ and the determinant of this equation is given by

$$\begin{aligned} & [(\mu + \lambda)(\lambda - p + \zeta\Theta) + \bar{q}^2] \times \\ & (\lambda - p_t + \zeta\Theta)^2 A^2 B^2 C^4 = 0. \end{aligned} \quad (74)$$

Thus, one of the solutions of the equation (74) is

$$[(\mu + \lambda)(\lambda - p + \zeta\Theta) + \bar{q}^2] = 0, \quad (75)$$

which can be rewritten as

$$\lambda^2 + (\mu - p + \zeta\Theta)\lambda + \bar{q}^2 - \mu(p - \zeta\Theta) = 0. \quad (76)$$

The two roots of the equation (76) are

$$\lambda_0 = -\frac{1}{2}(\mu - p + \zeta\Theta + \Delta), \quad (77)$$

and

$$\lambda_1 = -\frac{1}{2}(\mu - p + \zeta\Theta - \Delta), \quad (78)$$

where

$$\Delta^2 = (\mu + p - \zeta\Theta)^2 - 4\bar{q}^2 \geq 0, \quad (79)$$

must be greater or equal to zero in order to have real solutions. This equation can be rewritten as

$$|\mu + p - \zeta\Theta| - 2|\bar{q}| \geq 0. \quad (80)$$

The second solution of the equation (74) is

$$(\lambda - p_t + \zeta\Theta)^2 = 0, \quad (81)$$

whose roots are given by

$$\lambda_2 = \lambda_3 = p_t - \zeta\Theta. \quad (82)$$

A. Weak Energy Conditions

From equations (68) and (77) we get the first weak energy condition written as

$$\mu - p + \zeta\Theta + \Delta \geq 0. \quad (83)$$

From equation (69), setting $i = 1$ and using equations (77) and (78) we get the second weak energy condition given by

$$\Delta \geq 0, \quad (84)$$

which is equal to the condition (79).

From equation (69), now setting $i = 2, 3$ (since $\lambda_2 = \lambda_3$) and using equations (77) and (82) we get the third weak energy condition given by

$$\mu - p + 2p_t - \zeta\Theta + \Delta \geq 0. \quad (85)$$

B. Dominant Energy Conditions

From equation (70), setting $i = 1$ and using equations (77) and (78) we get the inequality

$$-(\mu - p + \zeta\Theta + \Delta) \leq -(\mu - p + \zeta\Theta - \Delta) \leq \mu - p + \zeta\Theta + \Delta, \quad (86)$$

which can be split into two inequalities, given by

$$\Delta \geq 0, \quad (87)$$

and

$$\mu - p + \zeta\Theta \geq 0. \quad (88)$$

From equation (70), setting $i = 2, 3$ and using equations (77) and (82) we get the inequality

$$-(\mu - p + \zeta\Theta + \Delta) \leq 2(p_t - \zeta\Theta) \leq \mu - p + \zeta\Theta + \Delta, \quad (89)$$

which again we can split it into two inequalities, given by

$$\mu - p + 2p_t - \zeta\Theta + \Delta \geq 0, \quad (90)$$

and

$$\mu - p - 2p_t + 3\zeta\Theta + \Delta \geq 0. \quad (91)$$

C. Strong Energy Conditions

Substituting equations (77), (78) and (82) into equation (71) we get the first strong energy condition given by

$$2p_t - 2\zeta\Theta + \Delta \geq 0. \quad (92)$$

Since one of the weak energy conditions, equation (69), is the same for the strong energy condition [equation (72)], thus we have that the second and third strong energy conditions are equal to equations (84)-(85), given by

$$\Delta \geq 0, \quad (93)$$

and

$$\mu - p + 2p_t - \zeta\Theta + \Delta \geq 0. \quad (94)$$

D. Summary of the Energy Conditions

Summarizing the results, we rewrite the energy conditions. The energy conditions for a spherically symmetric fluid whose energy-momentum tensor is given by equation (3) are fulfilled if the following inequalities are satisfied:

$$(i) \quad |\mu + p - \zeta\Theta| - 2|\bar{q}| \geq 0, \quad (95)$$

$$(ii) \quad \mu - p + 2p_t + \Delta - \zeta\Theta \geq 0, \quad (96)$$

and besides,

a) for the weak energy conditions

$$(iii) \quad \mu - p + \Delta + \zeta\Theta \geq 0, \quad (97)$$

b) for the dominant energy conditions

$$(iv) \quad \mu - p + \zeta\Theta \geq 0, \quad (98)$$

$$(v) \quad \mu - p - 2p_t + \Delta + 3\zeta\Theta \geq 0, \quad (99)$$

c) for the strong energy conditions

$$(vi) \quad 2p_t + \Delta - 2\zeta\Theta \geq 0, \quad (100)$$

where $\Delta = \sqrt{(\mu + p - \zeta\Theta)^2 - 4\bar{q}^2}$.

In order to verify the energy conditions, we have plotted the time evolution of all the conditions, for several radii and for two values of ζ (0 and 1000), as we can see in the figures 9, 10 and 11. For the sake of comparison with the model $\zeta \neq 0$, we have plotted all the conditions (95)-(100) for $\zeta = 0$.

From the figures 9(i) and 10(i) we can conclude that only the inequality $[|\mu + p - \zeta\Theta| - 2|\bar{q}| \geq 0]$ is not satisfied during all the collapse and for any radius. This inequality is not satisfied for the innermost radii ($r \leq 0.2r_\Sigma$) and for the latest stages of the collapse. The condition (100) is not satisfied for $r < 0.2r_\Sigma$ [figure 11(vi)] because the inequality (95) $[\Delta \geq 0]$ is not satisfied for these radii and for the latest stages of the collapse.

VII. PHYSICAL RESULTS

As in previous papers [6, 7, 9, 10, 12], we have calculated several physical quantities, as the total energy entrapped inside the Σ surface, the total luminosity perceived by an observer at rest at infinity and the effective adiabatic index, and we have compared them to the respective non-viscous ones.

From equation (35) we can write using (44)-(46) and (61)-(66) that

$$\frac{m}{m_0} = \frac{f}{16r_\Sigma^6(1-r_\Sigma^2)h^2} \left[m_0^2(1+r_\Sigma^2)^8 f^2 h^2 + 4r_\Sigma^4(1-r_\Sigma^4)^2(h^2-f^2) + 16r_\Sigma^6(1-r_\Sigma^2)^2 f^2 \right], \quad (101)$$

where

$$m_0 = - \left[r^2 B'_0 + \frac{r^3 B_0'^2}{2B_0} \right]_\Sigma. \quad (102)$$

We can see from figure 12 that the total energy entrapped inside the hypersurface Σ vanishes at the time -2.0×10^{-5} s, approximately. This means that the star radiates all its mass during the collapse and this explains why the apparent horizon never forms. We can

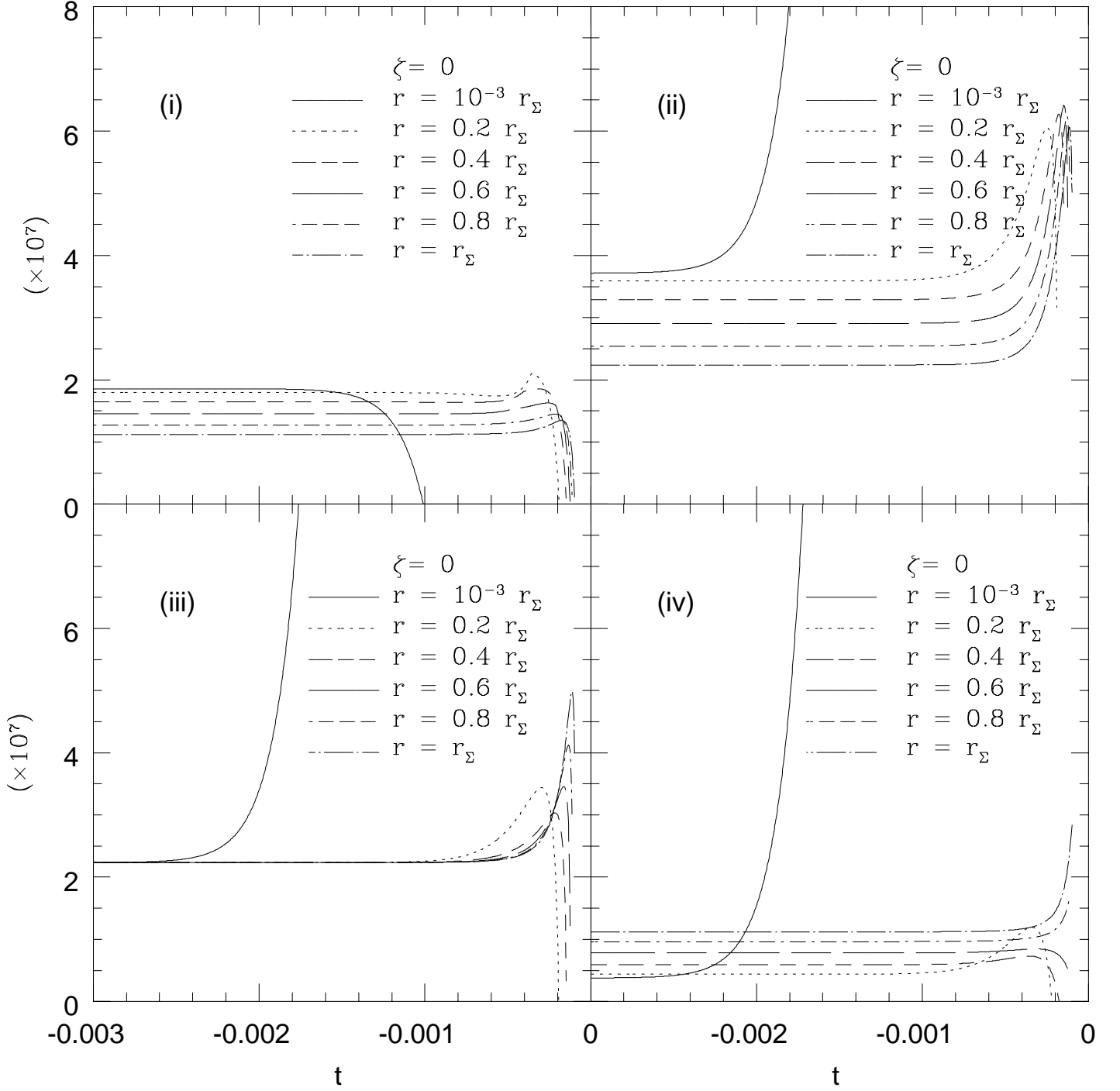


FIG. 9: The energy conditions (95)-(98), for the model without bulk viscosity, where $\zeta = 0$. The time is in units of seconds and all the others quantities are in units of sec^{-2} .

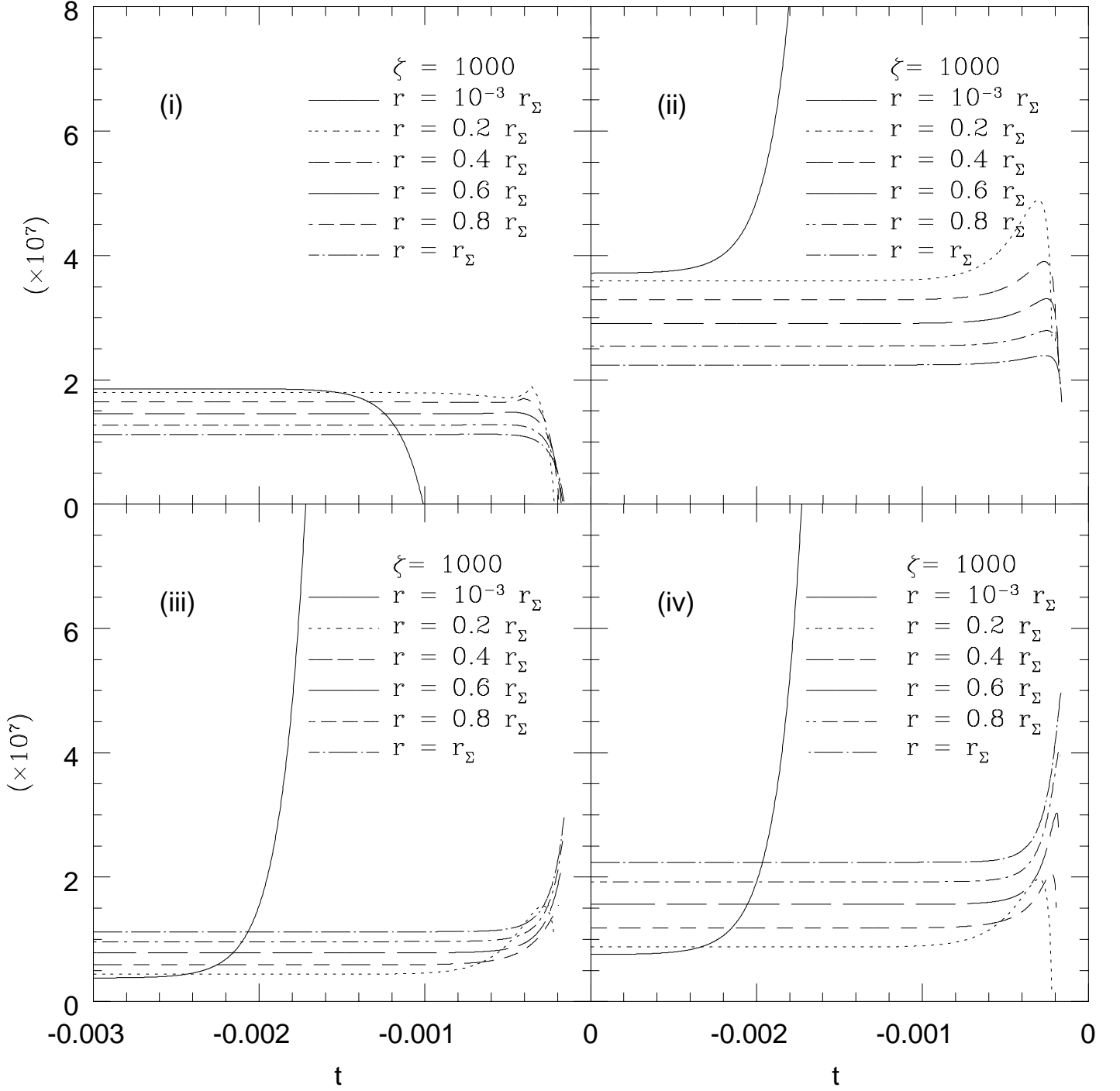


FIG. 10: The energy conditions (95)-(98), for the model without bulk viscosity, where $\zeta = 1000$.

The time is in units of seconds and all the others quantities are in units of sec^{-2} .

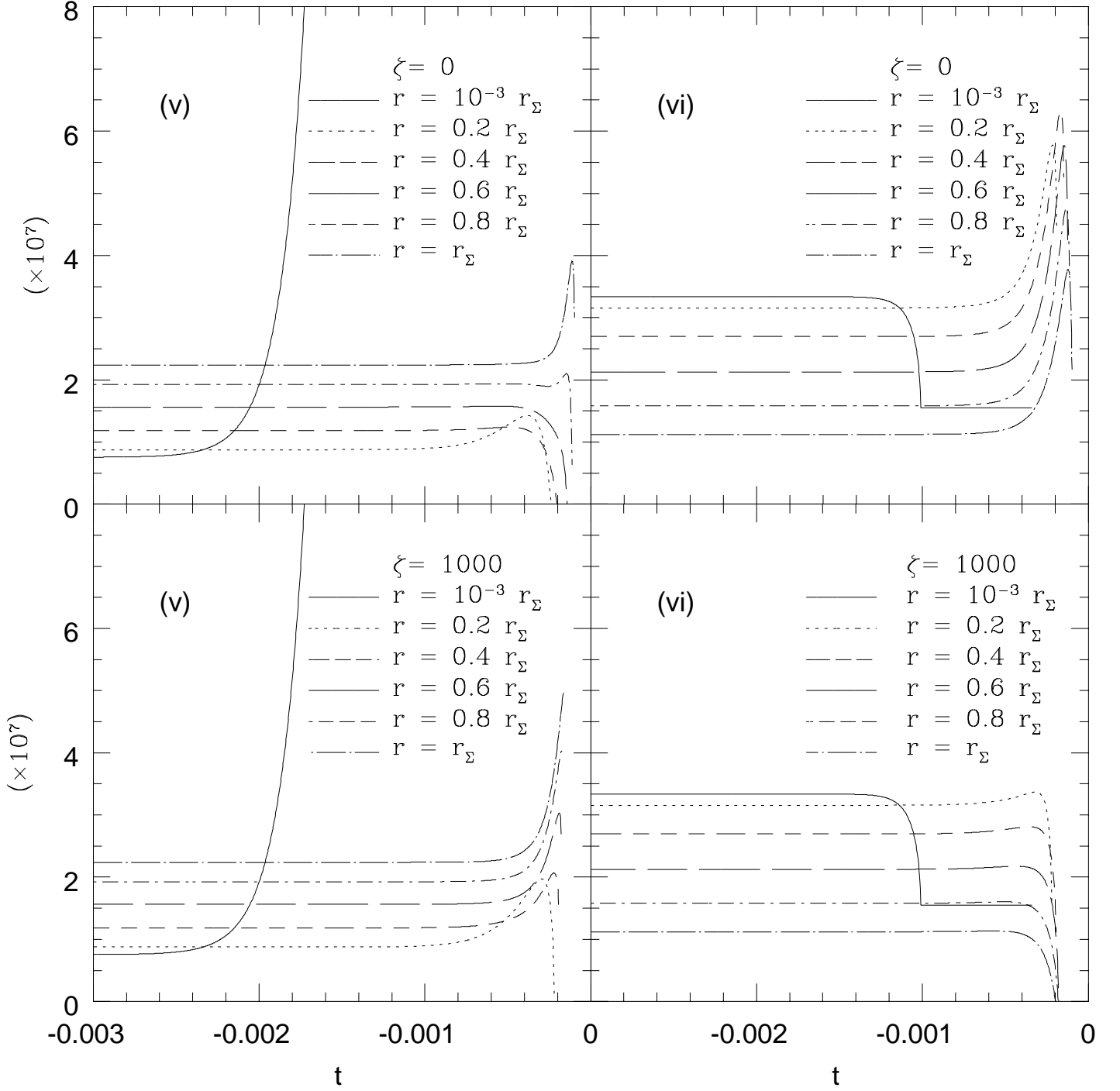


FIG. 11: The energy conditions (99)-(100), for the model with or without bulk viscosity, where $\zeta = 0$ and $\zeta = 1000$. The time is in units of seconds and all the others quantities are in units of sec^{-2} .

also observe from figure 12 that the mass inside Σ is equal for both models, with or without bulk viscosity. This means that they radiate the same amount of mass during the evolution. In the figure 13 we can see the evolution of the mass from a previous model [10]. In contrast of the result of this work, the former model radiates about 33% of the total mass of the star, before the formation of the black hole.

Using the equations (41) and (44)-(46) we can write the luminosity of the star as

$$L_\infty = \kappa \frac{m_0^2(1+r_\Sigma^2)^4 f^2}{8r_\Sigma^4} \times \left[\left(\frac{1-r_\Sigma^2}{1+r_\Sigma^2} \right) \left(\frac{f}{h} \right) + \frac{m_0(1+r_\Sigma^2)^3 \dot{f}}{2r_\Sigma^2(1-r_\Sigma^2)} \right]^2 \left[p_\Sigma - \zeta \left(\frac{1+r_\Sigma^2}{1-r_\Sigma^2} \right) \left(2\frac{\dot{f}}{f} + \frac{\dot{h}}{h} \right) \right]. \quad (103)$$

We can see from figure 14 that the luminosity perceived by an observer at rest at infinity increases exponentially until the time -2.0×10^{-5} , when the total mass of the star vanishes. In the figure 15 we can see the evolution of the luminosity from a previous model [10]. In contrast of the result of this work, the luminosity of the star also increases exponentially, reaching a maximum and after it decreases until the formation of the black hole.

The effective adiabatic index can be calculated using the equations (48)-(49), (60) and (61)-(66). Thus, we can write that

$$\begin{aligned} \Gamma_{\text{eff}} &= \left[\frac{\partial(\ln p)}{\partial(\ln \mu)} \right]_{r=\text{const}} = \left(\frac{\dot{p}}{\dot{\mu}} \right) \left(\frac{\mu}{p} \right) = \\ &= \left\{ \left[288r^2 e(r) + 12d(r)k(r) \right] f^2 + 6ac(r)k(r)h f \dot{f} - 6\kappa\zeta A_0 c(r)k(r)(h^3 + h)f^2/a_0 \right\} f \dot{h} + \\ &\quad + c(r)k(r)j(r,t)f \left[3h^2 \dot{f}^2 + bh^2(1-f^2) \right] + \\ &\quad + k(r)h \dot{f} \left[c(r)(12bh^2 + aj(r,t)f^2) - 12d(r)h^2 \right] \} \times \\ &\quad \times 2^{-1} \left\{ \left[24r^2 d(r)f^2 + k(r) \left[c(r)(3h^2 \dot{f}^2 + afh \dot{f} + bh^2(1-f^2)) - \right. \right. \right. \\ &\quad \left. \left. \left. - 2d(r)f^2 \right] \right\} f \dot{h} + c(r)k(r)(3h^3 \dot{f}^3 + ah^2 f \dot{f}^2) + \right. \\ &\quad \left. + k(r) \dot{f} \left[bc(r)h^3(1-f^2) + 2d(r)h^3 \right] - 2c(r)k(r)f^2 \dot{f} h \dot{h} (1+h^2)/a_0 \right\}^{-1} \times \\ &\quad \times \left\{ 12r^2 d(r)f^2 + k(r) \left[c(r)h^2 \dot{f}^2 + d(r)(h^2 - f^2) \right] + \right. \\ &\quad \left. + 2c(r)k(r)f \dot{f} h \dot{h} \right\} \times \end{aligned}$$

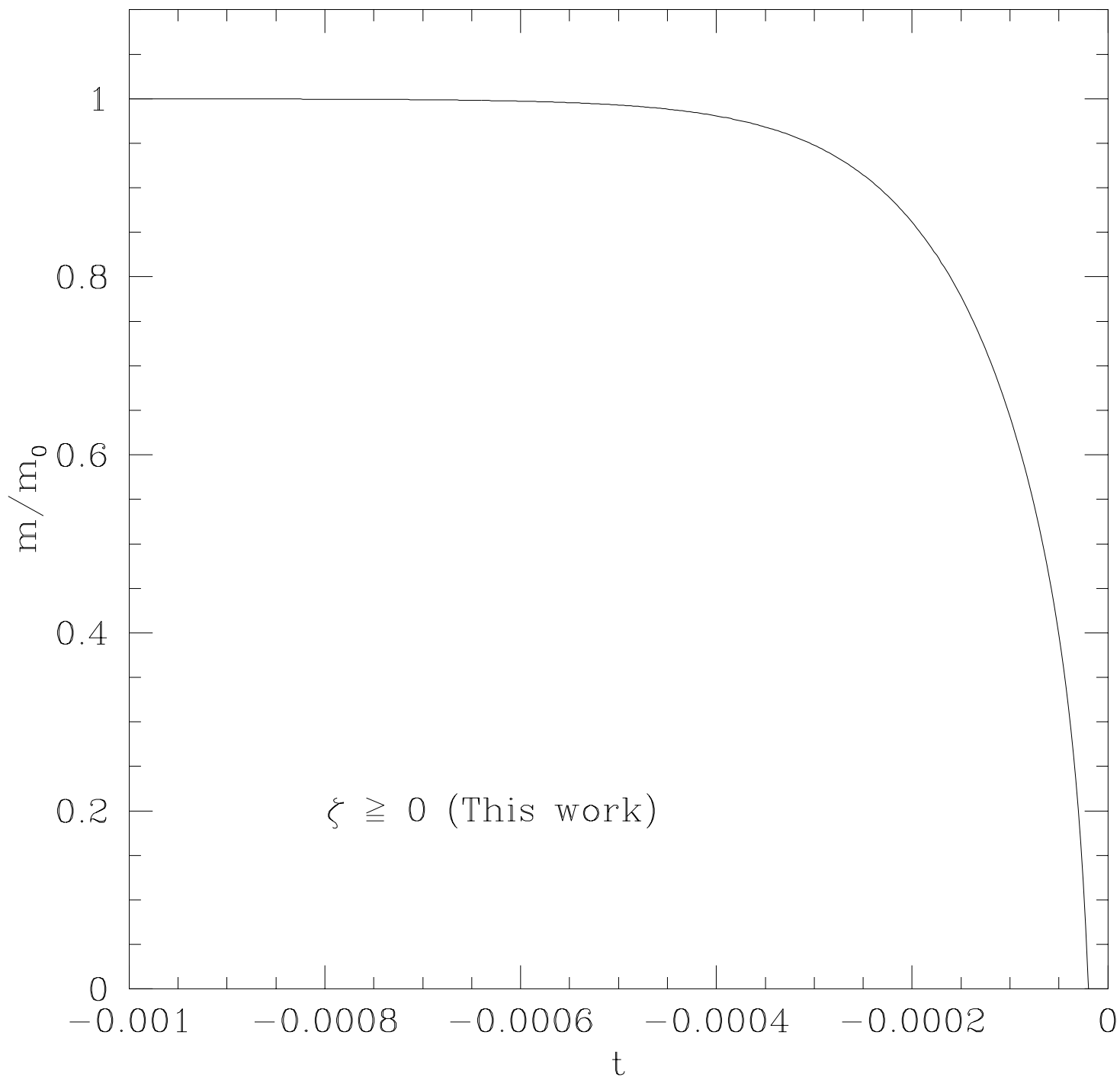


FIG. 12: Time behavior of the total energy entrapped inside the surface Σ for the models with or without bulk viscosity. The time, m and m_0 are in units of seconds. The symbols $\zeta \geq 0$ mean that the plotted quantity is independent of ζ .

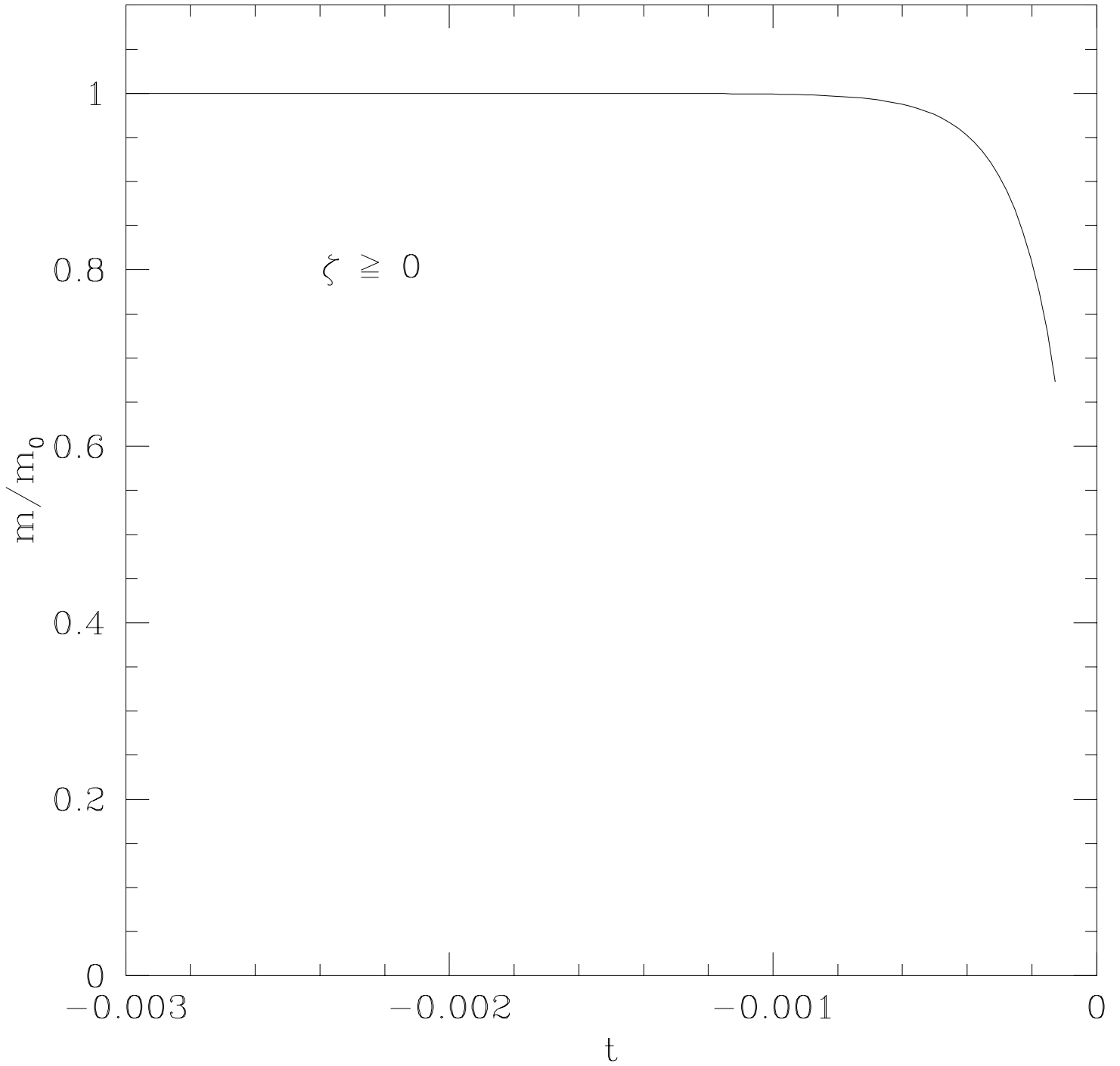


FIG. 13: Time behavior of the total energy entrapped inside the surface Σ for the models with or without bulk viscosity, from a previous model [10]. The time, m and m_0 are in units of seconds. The symbols $\zeta \geq 0$ mean that the plotted quantity is independent of ζ .

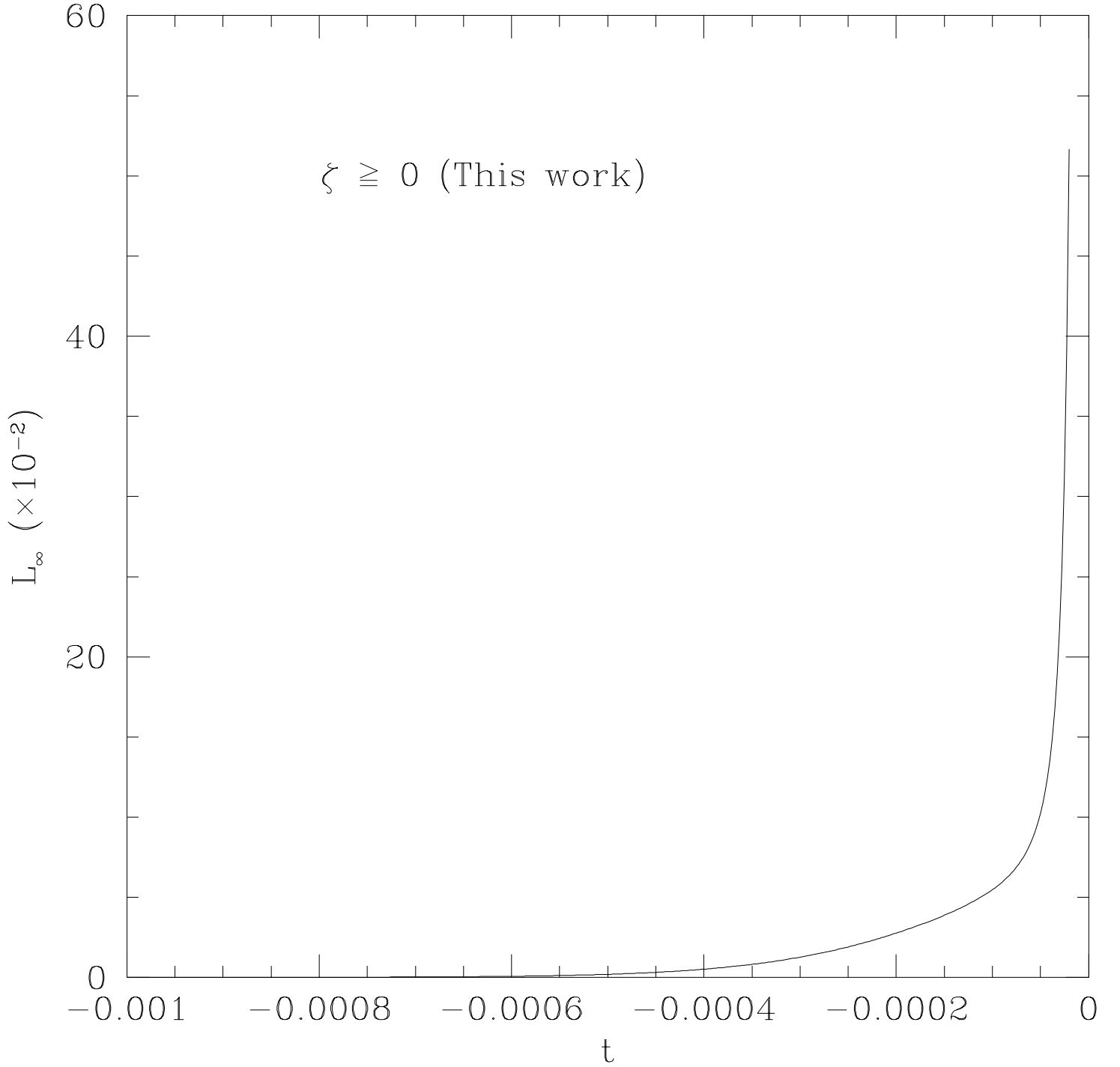


FIG. 14: Time behavior of the luminosity perceived by an observer at rest at infinity for the models with or without bulk viscosity. The time is in units of second and the luminosity is dimensionless. The symbols $\zeta \geq 0$ mean that the plotted quantity is independent of ζ .

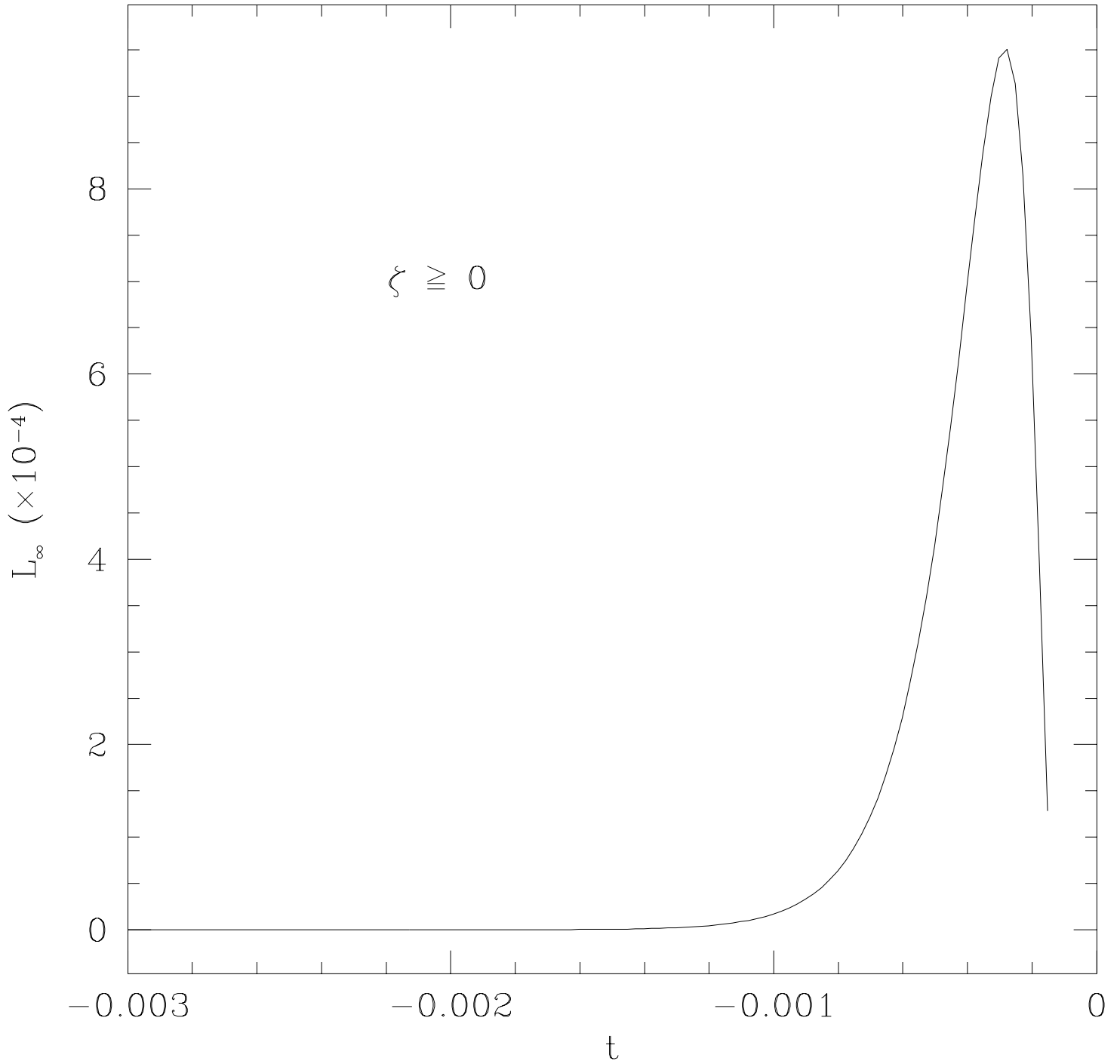


FIG. 15: Time behavior of the luminosity perceived by an observer at rest at infinity for the models with or without bulk viscosity, from a previous model [10]. The time is in units of second and the luminosity is dimensionless. The symbols $\zeta \geq 0$ mean that the plotted quantity is independent of ζ .

$$\begin{aligned} & \times \left\{ 72r^2 e(r) f^2 + k(r) \left\{ c(r) j(r, t) h f \dot{f} + 3[c(r)b - d(r)] \times \right. \right. \\ & \quad \left. \left. \times (h^2 - f^2) \right\} - c(r) k(r) l(r, t) f^2 \dot{h} \right\}^{-1}, \end{aligned} \quad (104)$$

where

$$c(r) = r^2 m_0^2 (1 + r_\Sigma^2)^8, \quad (105)$$

$$d(r) = r_\Sigma^6 g^2(r), \quad (106)$$

$$e(r) = r_\Sigma^6 (r_\Sigma^2 - r^2) g(r), \quad (107)$$

$$k(r) = (1 + r^2)^2, \quad (108)$$

$$j(r, t) = 3a + 6\kappa\zeta A_0 h. \quad (109)$$

and

$$l(r, t) = 3a_o b - 3\kappa\zeta A_0 h. \quad (110)$$

Comparing the figures for Γ_{eff} ($\zeta = 0$ and $\zeta \neq 0$) we can see that the time evolution of the effective adiabatic indices are not very different graphically. This is the reason to plot the quantity $\delta\Gamma = \Gamma_{\text{eff}}(\zeta = 0) - \Gamma_{\text{eff}}(\zeta \neq 0)$ instead of Γ_{eff} for the $\zeta \neq 0$ models. We can note in figure 16 ($\zeta = 0$) that shortly before the peak of luminosity (see figure 14) there is a large discontinuity in Γ_{eff} due mainly to the behavior of the pressure. The effect of the viscosity is to increase much more these discontinuities.

In the figure 17 we can see the evolution of the effective adiabatic indices from a previous model [10]. We can note comparing it with the figure 16 that the effective adiabatic index diminishes due to the bulk viscosity, thus increasing the instability of the system, in both models, in the former paper [10] and in this work. This characteristic might be model independent.

Finally, models of radiating viscous spheres have been presented by Herrera, Jiménez and Barreto [26]. This work is particularly relevant for the proposed discussion because the conclusion concerning the effective adiabatic index is the same in both cases. Namely, an increasing of the critical adiabatic index required for stability [27], or equivalently, a decreasing of the effective adiabatic index, induced by viscosity. Since the models considered in each case are completely different, we suggest that this effect seems to be model independent.

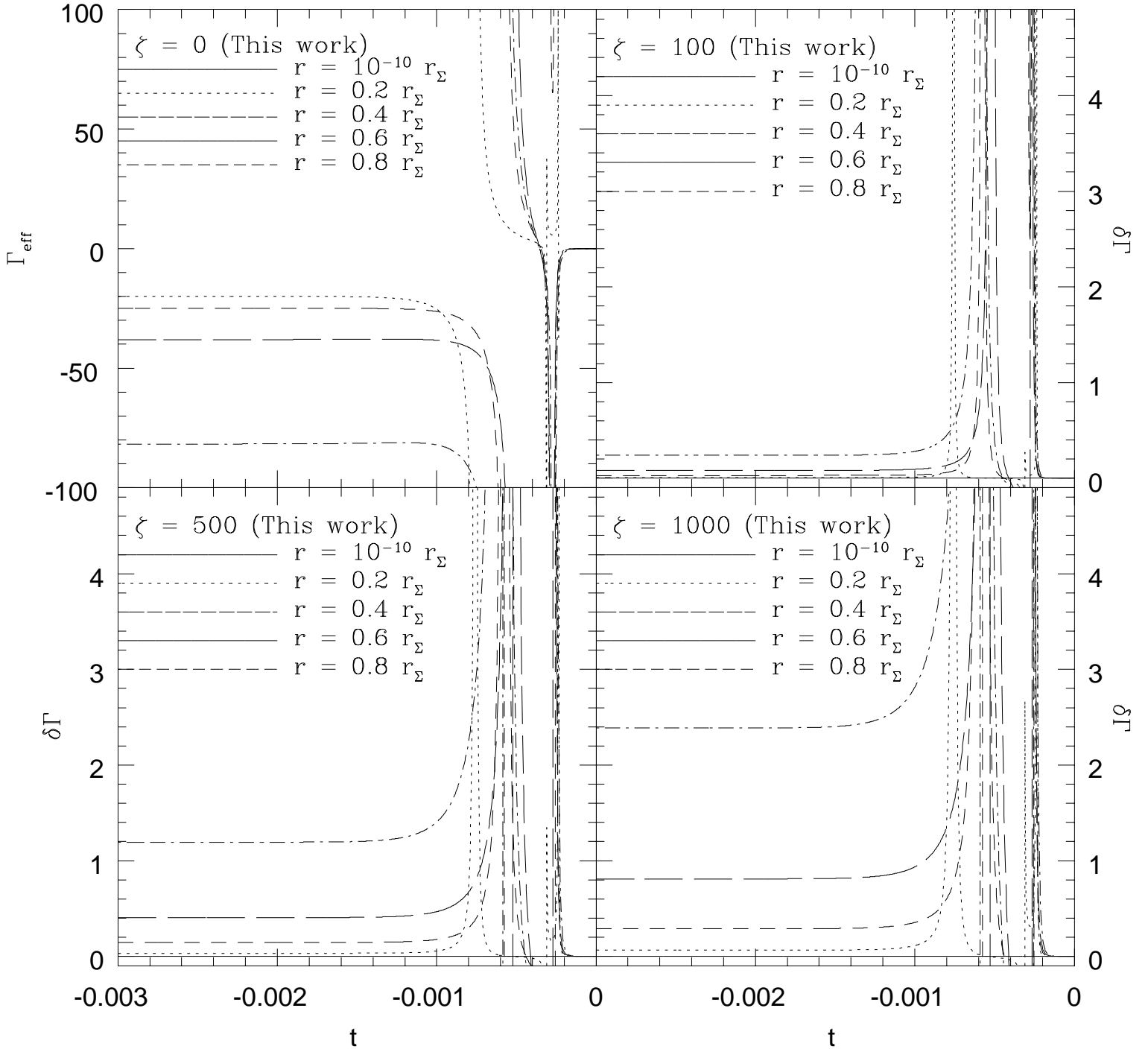


FIG. 16: Time behavior of the effective adiabatic index Γ_{eff} for four values of ζ . The quantity $\delta\Gamma$ is defined as $\Gamma_{\text{eff}}(\zeta = 0) - \Gamma_{\text{eff}}(\zeta \neq 0)$. The time is in units of seconds, Γ_{eff} and $\delta\Gamma$ are dimensionless.

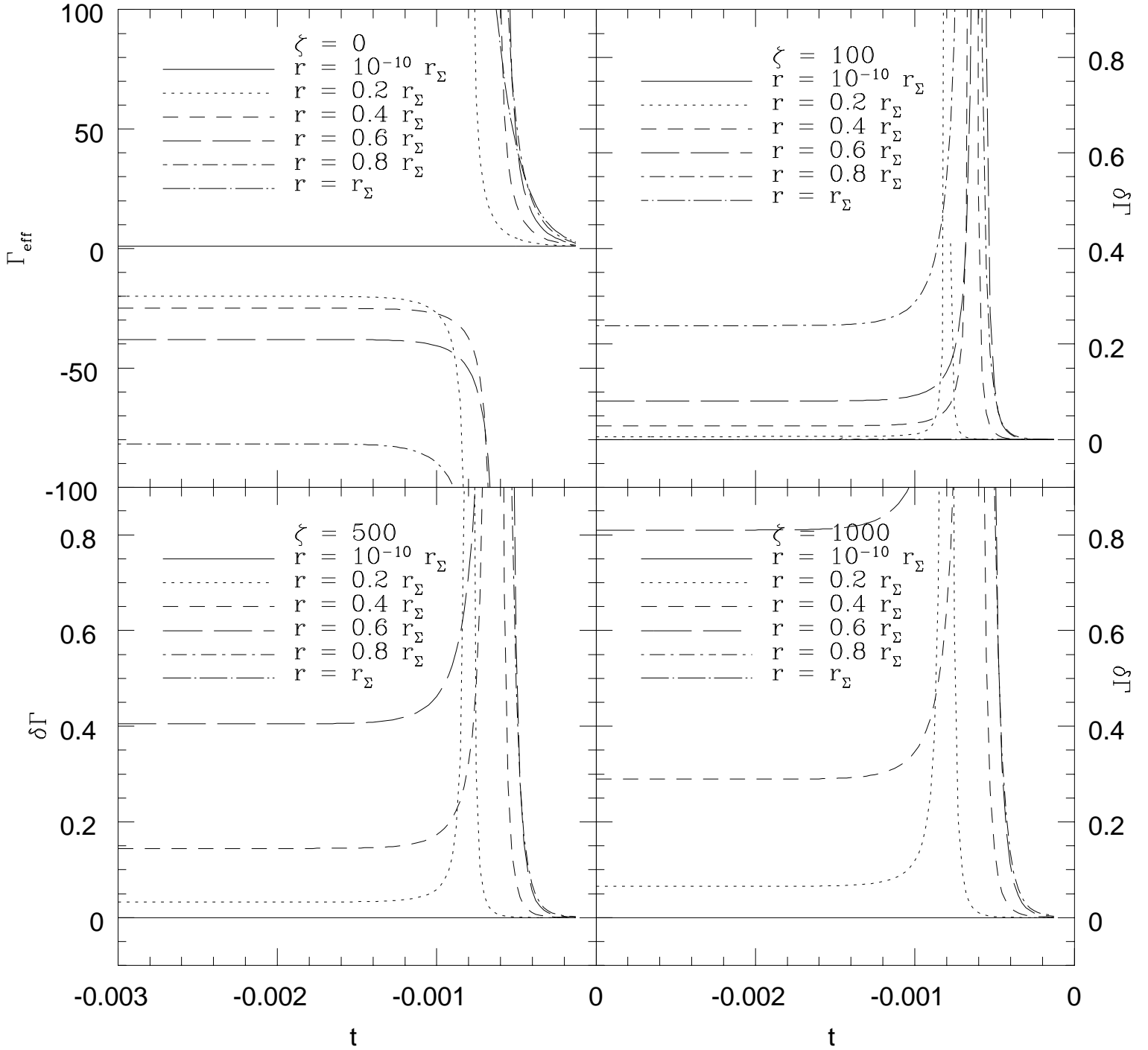


FIG. 17: Time behavior of the effective adiabatic index Γ_{eff} for four values of ζ , from a previous model [10]. The quantity $\delta\Gamma$ is defined as $\Gamma_{\text{eff}}(\zeta = 0) - \Gamma_{\text{eff}}(\zeta \neq 0)$. The time is in units of seconds, Γ_{eff} and $\delta\Gamma$ are dimensionless.

VIII. CONCLUSIONS

A new model is proposed to a collapsing star consisting of an anisotropic fluid with bulk viscosity, radial heat flow and outgoing radiation. In a previous paper [11] one of us has introduced a function time dependent into the g_{rr} , besides the time dependent metric functions $g_{\theta\theta}$ and $g_{\phi\phi}$. We have generalized this previous model by introducing bulk viscosity and we have compared it to the non-viscous collapse.

The behavior of the density, pressure, mass, luminosity and the effective adiabatic index was analyzed. We have also compared to the case of a collapsing fluid with bulk viscosity of another previous model [10], for a star with $6 M_{\odot}$.

As we have shown the black hole is never formed because the apparent horizon formation condition is never satisfied. This could be interpreted as the formation of a naked singularity, as Joshi, Dadhich and Maartens [14] have suggested. However this is not the case because the star radiates all its mass before it reaches the singularity at $r = 0$ and $t = 0$. Not even a marginally naked singularity is formed by the same reason, since in this case the apparent horizon should coincide with the singularity at $r = 0$ and $t = 0$.

The density and pressure have negative values although physically this could be considered unreasonable. However, due to the heat flow (the term Δ) the energy conditions are partially satisfied.

The pressure of the star, at the beginning of the collapse, is isotropic but due to the presence of the bulk viscosity the pressure becomes more and more anisotropic.

The star radiates all its mass during the collapse and this explains why the apparent horizon never forms. In contrast of the result of this work, the former model radiates about 33% of the total mass of the star, before the formation of the black hole.

An observer at infinity will see a radial point source radiating exponentially until reaches the time of maximum luminosity and suddenly the star turns off because there is no more mass in order to be radiated. In contrast of the former model [10] where the luminosity also increases exponentially, reaching a maximum and after it decreases until the formation of the black hole.

The effective adiabatic index has a very unusual behavior because we have a non-adiabatic regime in the fluid due to the heat flow. The index becomes negative since the hydrodynamic pressure and the density may become negative. Besides, in this case, neither the density is

the measure of the total energy density of a given piece of matter nor the hydrodynamic pressure the only opposing contraction [28]. The effective adiabatic index diminishes due to the bulk viscosity, thus increasing the instability of the system, in both models, in the former paper [10] and in this work, showing that this characteristic might be model independent.

ACKNOWLEDGMENTS

The author (RC) acknowledges the financial support from FAPERJ (no. E-26/171.754/2000, E-26/171.533/2002 and E-26/170.951/2006) and from Conselho Nacional de Desenvolvimento Científico e Tecnológico - CNPq - Brazil. The author (GP) also acknowledges the financial support from CAPES.

-
- [1] de Oliveira, A.K.G., Santos, N.O., Kolassis, C.A., *Mon. Not. R. Astron. Soc.*, 216, 1001 (1985).
 - [2] Bonnor, W.B., de Oliveira, A.K.G., Santos, N.O., *Phys. Rep.*, 181, 269 (1989).
 - [3] Chan, R., *Astrophys. J.* 342, 976 (1989).
 - [4] Chan, R., *Astrophys. Spa. Sci.* 206, 219 (1993).
 - [5] Martínez, J., Pavón, D., *Mon. Not. R. Astron. Soc.*, 268, 654 (1994).
 - [6] Chan, R., *Mon. Not. R. Astron. Soc.* 288, 589 (1997).
 - [7] Chan, R., *Mon. Not. R. Astron. Soc.* 299, 811 (1998).
 - [8] Chan, R., *Astrophys. Spa. Sci.* 257, 299 (1998).
 - [9] Chan, R., *Mon. Not. R. Astron. Soc.* 316, 588 (2000).
 - [10] Chan, R., *Astron. Astrophys.* 368, 325 (2001).
 - [11] Chan, R., *Int. J. Mod. Phys. D* 12, 1131 (2003).
 - [12] Nogueira, P.C. and Chan, R., *Int. J. Mod. Phys. D* 13, 1727 (2004).
 - [13] Pinheiro, G. and Chan, R. 2008, *Gen. Rel. Grav.* 40, 2149 (2008).
 - [14] Joshi, P.S., Dadhich, N. and Maartens, R., *Phys. Rev. D* 65, 101 501 (2002).
 - [15] Herrera, L., Santos, N.O., *Phys. Rep.*, 286, 53 (1997).
 - [16] Vaidya, P.C., *Nature*, 171, 260 (1953).
 - [17] Israel, W., *Nuovo Cimento*, 44B, 1 (1966).
 - [18] Israel, W., *Nuovo Cimento*, 48B, 463 (1966).
 - [19] Santos, N.O., *Mon. Not. R. Astron. Soc.*, 216, 403 (1985).

- [20] Cahill, M.E., McVittie G.C., *J. Math. Phys.*, 11, 1382 (1970).
- [21] Raychaudhuri, A.K., Maiti, S.R., *J. Math. Phys.*, 20, 245 (1979).
- [22] Woosley, S.E., Phillips, M.M., *Science*, 240, 750 (1988).
- [23] Cutler, C. and Lindblom, L., *Astrophys. J.* 314, 234 (1987).
- [24] Anderson, N., Comer, G. L. and Glampedakis, K., *Nucl. Phys. A* 763, 212 (2005).
- [25] Kolassis, C.A., Santos, N.O., Tsoubelis, D., *Class. Quantum Grav.*, 5, 1329 (1988).
- [26] Herrera, L., Jiménez, J. and Barreto, W., *Can. J. Phys.* 67, 855 (1989).
- [27] Chan, R., Herrera, L., Santos, N.O., *Mon. Not. R. Astron. Soc.*, 267, 637 (1994).
- [28] Barreto, W., Herrera, L. and Santos, N.O., *Astrophys. Spa. Sci.* 187, 271 (1992).